2012

Impact of E22 on two-stroke and four-stroke snowmobiles

James Corey Weber

Michigan Technological University

Recommended Citation

IMPACT OF E22 ON TWO-STROKE AND FOUR-STROKE SNOWMOBILES

By

James Corey Weber

A THESIS

Submitted in partial fulfillment of the requirements for the degree of

MASTER OF SCIENCE

(Mechanical Engineering)

MICHIGAN TECHNOLOGICAL UNIVERSITY

2012

This thesis, "Impact of E22 on Two-Stroke and Four-Stroke Snowmobiles," is hereby approved in partial fulfillment of the requirements for the Degree of MASTER OF SCIENCE IN MECHANICAL ENGINEERING.

Department of Mechanical Engineering-Engineering Mechanics

Signatures:

Thesis Advisor   _____

Dr. Scott A. Miers

Department Chair   _____

Dr. William W. Predebon

Date   _____

Table of Contents

List of Figures

6

8

List of Tables

9

Nomenclature

AFR: Air to Fuel Ratio

BMEP: Brake Mean Effective Pressure

BSFC: Brake Specific Fuel Consumption

CFM: Cubic Feet per Minute

CO: Carbon Monoxide

CO_2: Carbon Dioxide

EGT: Exhaust Gas Temperature

EISA: Energy Independence and Security Act

Exx: xx Volume Percent of Ethanol

IMEP: Indicated Mean Effective Pressure

Lambda: Relative Air to Fuel Ratio (λ)

LTFT: Long Term Fuel Trim

MBT: Minimum spark advance for Best Torque

MFB: Mass Fraction Burned

NMHC: Non-Methane HydroCarbons

NMOG: Non-Methane Organic Gas

NO_x: Oxides of Nytrogen

O_2: Diatomic Oxygen

RFS: Renewable Fuel Standard

RON: Research Octane Number

THC: Total HydroCarbons

WOT: Wide Open Throttle

Abstract

A push to reduce dependency on foreign energy and increase the use of renewable energy has many gas stations pumping ethanol blended fuels. Recreational engines typically have less complex fuel management systems than that of the automotive sector. This prevents the engine from being able to adapt to different ethanol concentrations. Using ethanol blended fuels in recreational engines raises several consumer concerns. Engine performance and emissions are both affected by ethanol blended fuels.

This research focused on assessing the impact of E22 on two-stroke and four-stroke snowmobiles. Three snowmobiles were used for this study. A 2009 Arctic Cat Z1 Turbo with a closed-loop fuel injection system, a 2009 Yamaha Apex with an open-loop fuel injection system and a 2010 Polaris Rush with an open-loop fuel injection system were used to determine the impact of E22 on snowmobile engines. A five mode emissions test was conducted on each of the snowmobiles with E0 and E22 to determine the impact of the E22 fuel. All of the snowmobiles were left in stock form to assess the effect of E22 on snowmobiles currently on the trail.

Brake specific emissions of the snowmobiles running on E22 were compared to that of the E0 fuel. Engine parameters such as exhaust gas temperature, fuel flow, and relative air to fuel ratio (λ) were also compared on all three snowmobiles. Combustion data using an AVL combustion analysis system was taken on the Polaris Rush. This was done to compare in-cylinder pressures, combustion duration, and location of 50% mass fraction burn.

E22 decreased total hydrocarbons and carbon monoxide for all of the snowmobiles and increased carbon dioxide. Peak power increased for the closed-loop fuel injected Arctic Cat. A smaller increase of peak power was observed for the Polaris due to a partial ability of the fuel management system to adapt to ethanol. A decrease in peak power was observed for the open-loop fuel injected Yamaha.

Chapter 1 Introduction

There is a need to understand the impact of ethanol blended fuels on recreational engines. As ethanol concentrations increase at the pump, it is becoming more difficult to find non-oxygenated fuel for recreational engines. This thesis focuses on snowmobile engines and the impact from higher ethanol content fuel. To help keep purchase prices low, many snowmobile engines are less complex than automotive fuel management systems. This prevents snowmobile engines from being able to adapt to ethanol blended fuels. This inability to adapt raises two major concerns of running ethanol blended fuels. One concern is the effect on emissions. As ethanol concentration increases, combustion tends to go lean. This leaning effect increases cylinder temperatures which can affect emissions and overall engine durability. The second concern is the impact of ethanol blended fuels on engine performance. Ethanol has a decreased heating value when compared to gasoline which results in decreased power output.

1.1 Renewable Fuel Standard (RFS)

The Energy Policy Act (EPAct) of 2005 created the RFS program. The first stage of the RFS program was to blend 7.5 billion[1] gallons of renewable fuel into gasoline by 2012. The second stage of the RFS program was set into place by the Energy Independence and Security Act (EISA) of 2007. This stage required 36 billion[1] gallons of renewable fuel to be blended into transportation fuels including diesel. EISA created standards that require that new renewable fuels must emit fewer greenhouse gases than the fuel they replace. The RFS program also reduces the need for importing fuel and promotes the development of the renewable fuels sector.

1.2 Snowmobile statistics

With over 1.5 million snowmobiles registered nationwide[2] in 2011 it is important to consider how snowmobiles are affected by ethanol blended fuels. An estimated 51,796 new snowmobiles were sold in 2011 alone. The average rider rides their snowmobile 1414 miles per season on over 225,000 miles of groomed trails in North America.

1.3 Research Goal and Objectives

The research goal was to assess the impact of E22 (22 % by volume ethanol 78 % by volume gasoline) on snowmobile engines. The considered impacts were emissions, engine performance, and combustion parameters. Three snowmobiles with significantly different fuel management strategies were used for testing. One fuel management method was a closed-loop throttle body fuel injected four-stroke engine. This system was similar to modern automotive control systems. The second system was an open-loop port fuel injected four-stroke engine. The third snowmobile was an open-loop semi-direct injected two-stroke engine. Each of the snowmobiles were instrumented with thermocouples for exhaust gas temperatures, coolant temperatures, intake temperatures, and oil temperature for the four-stroke snowmobile. A Land and Sea nine inch water brake dynamometer was mounted to the crankshaft to provide load for emissions testing. A Re-sol fuel measurement cart was implemented to record fuel flow. A Horiba MEXA 1600D emissions analyzer was utilized to record raw emission concentrations. E0 and E22 fuel from Gage Products was used for emissions testing. An AVL combustion analysis package was used on the two-stroke snowmobile to record in-cylinder pressures on a crank angle basis.

A power sweep was conducted on each of the snowmobiles to determine the peak power and the engine speed where peak power occurred. The peak power engine speed and peak power torque was used to calculate a five mode emissions test. Tests were conducted in triplicate to assess repeatability of the results.

Chapter 2 Background/Literature Review

A demand for a renewable energy source to supplement or even replace gasoline has many fuel stations pumping gasoline-ethanol blends. In the performance world of snowmobiles, ethanol raises several concerns. These concerns include emissions and engine performance, as well as, the effect of ethanol on engines with less complex fuel management systems.

2.1 Literature Description

Due to limited testing of ethanol on snowmobile engines, this literature review focuses on the affects of ethanol-gasoline blends on internal combustion engines. The following sub-sections describe the engines used, ethanol concentrations, and test methods of the reviewed literature.

2.1.1 Ning et. al 2005, SAE 2005-32-0053[3]

For this paper, three different single cylinder, air cooled, carbureted motorcycles were used for testing. Included was a 100 cc four stroke, a 125 cc four stroke and a 100 cc two-stroke. There were three motorcycles of each model. One motorcycle was run using E0 while the other two were run with E10. Each motorcycle was tested at 1,000 km for emissions, maximum speed and fuel consumption at a constant speed. This process was then repeated after driving the motorcycles for a total of 10,000 km

2.1.2 Knoll et. al 2009, SAE 2009-01-2723[4]

For this study 16 production vehicles of model years 1999 to 2007 and 10,000 to 100,000 miles on the odometer were used for testing. Four fuels were used: E0, E10, E15 and E20. Emissions were found using the LA92 drive cycle[5]. Some of the vehicles had a long term fuel trim (LTFT) which allowed the vehicle to learn the fuel and make adjustments for the ethanol content.

2.1.3 Nakata et. al 2006, SAE 2006-01-3380[6]

For this study, an automotive application Toyota engine was used. The engine was an inline four cylinder four-stroke with multi port fuel injection and a displacement of 1496 cc. The engine's compression ratio was increased to 13 from the production 10.5. The fuels used for this test were a 100 research octane number (RON) gasoline, and a 92 RON gasoline. Ethanol was then added to the 92 RON gasoline in concentrations of E10, E20, E50 and E100. Thermal efficiency, oxides of nitrogen (NOx), total hydrocarbons (THC), carbon dioxide (CO_2) and ignition timing were recorded at 2000 rpm and a brake mean effective pressure (BMEP) of 200 kPa for the different blends of ethanol. Volumetric efficiency, thermal efficiency, ignition timing, torque and brake specific fuel consumption (BSFC) were recorded at 2800 rpm and wide open throttle (WOT) for the different blends of ethanol. Cold start testing was also completed but due to the lack of cold start testing for the other studies, is ignored for this review.

2.1.4 Czerwinski et. al 2012, SAE 2010-01-0794[7]

For this paper, a 2004 two-stroke Piaggio Typhoon, a 1976 two-stroke Kreidler Florett and a 2004 four-stroke Honda Zoomer were used for testing. All of the scooters were single cylinder, 50 cc, carbureted engines. The Honda Zoomer was liquid cooled while the other two were air cooled. The fuels used for blending were 95 RON gasoline, pure ethanol and hydrous ethanol. The hydrous ethanol contained 4 % water by volume. The fuels were blended into concentrations of E0, E5, E10, E15, E20, EH5, EH10, EH15 and EH20. Drive cycles were determined using regulations of the Bundesamt für Umwelt, which is Switzerland's environmental protection agency.

2.2 Effect of Ethanol Blends on Emissions

Pure ethanol (E100) has a higher flame speed, shorter burn duration, larger latent heat of vaporization, smaller heating value, and a smaller stoichiometric air/fuel ratio than that of gasoline. These differences, as well as a different chemical composition directly affect emissions.

17

2.2.1 Ning et. al 2005, SAE 2005-32-0053

The use of E10 reduced carbon monoxide (CO) by 50 %. THC was reduced by 20 %. Figure 2.1 shows a consistent decrease in CO, however there is no trend in NOx. NOx varies from a nearly 30 % reduction to a nearly 80 % increase.
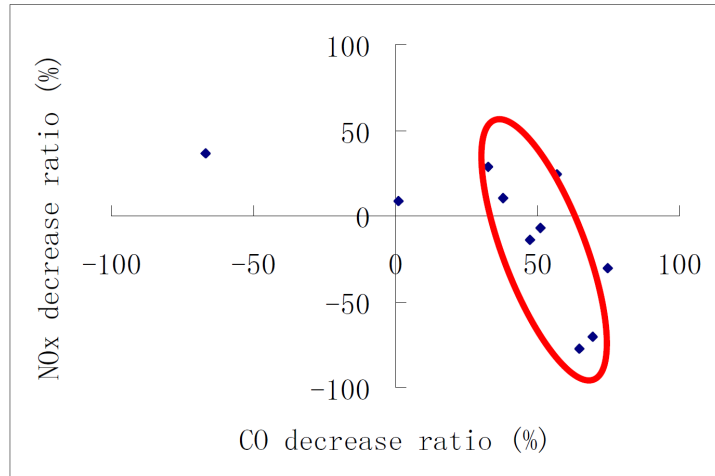
Figure 2.1[3]: Percent decrease of CO and NO_x for E10 compared to E0 with small displacement motorcycles.

Reprinted with permission from SAE Paper No. 2005-32-0053 © 2005 SAE International

2.2.2 Knoll et. al 2009, SAE 2009-01-2723

The emissions recorded for this study were: non-methane organic gas (NMOG), non-methane hydrocarbons (NMHC), CO, NOx, ethanol, acetaldehyde and formaldehyde. Fuel economy was also recorded. As shown in Figure 2.2, CO and NMHC were reduced when compared to E0. As the ethanol concentration increased from E10, changes in CO and NMHC are relatively constant. NOx emissions were increased in the vehicles that do not apply LTFT. The vehicles that do apply LTFT saw a decrease in NOx emissions. The decrease of NO_x in vehicles that apply LTFT was due to the vehicle's ability to adapt to the ethanol concentration in the fuel. During WOT and near WOT conditions, many automotive engines switch to an open-loop fuel strategy where more fuel is injected to reduce engine and exhaust temperatures. Vehicles that

applied LTFT still account for ethanol concentration during the open-loop mode and therefore maintained relative air/fuel ratio (λ). Maintaining λ caused a decrease in in-cylinder temperatures due to the larger latent heat of vaporization of ethanol. This decrease in temperature, in turn, reduced NO_x. Fuel economy decreased as ethanol concentration was increased for all vehicles.
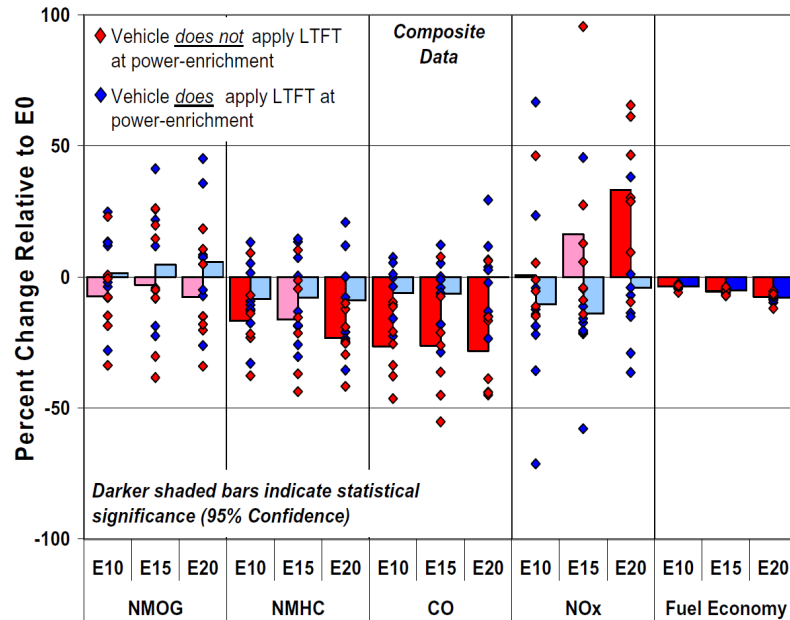
Figure 2.2[4]: Percent change of emissions relative to E0 with various automobiles.

Figure 2.3 shows that ethanol emissions were higher with the vehicles that did not apply LTFT. However, both types of vehicles observed an increase of ethanol in the exhaust. Acetaldehyde also increased as ethanol concentration increased. Formaldehyde increased statistically significantly for the vehicles that applied LTFT. The vehicles that did not apply LTFT did not have a statistically significant increase in Formaldehyde.
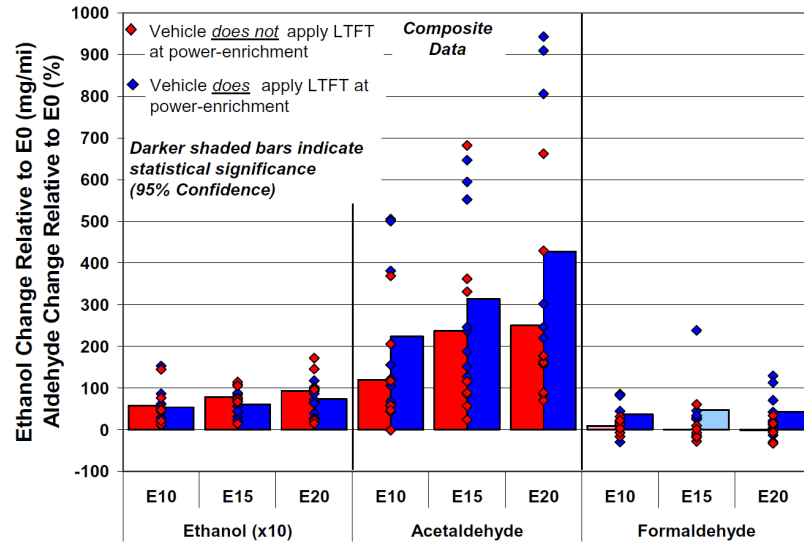
Figure 2.3[4]: Percent change of ethanol and aldehyde emissions relative to E0 with various automobiles.

2.2.3 Nakata et. al 2006, SAE 2006-01-3380

For each blend of ethanol, the ignition timing was set to the minimum spark advance for best torque (MBT). As the ethanol concentration was increased, the ignition timing could be retarded and still maintain maximum torque due to ethanol having a faster rate of combustion. As the ethanol concentration was increased, NOx, THC and CO_2 decreased (Figure 2.4). NOx emissions decreased from 16 g/kWh to 10 g/kWh. THC decreased from 7.5 g/kWh at E0 to 2 g/kWh at E100. CO_2 emissions increased from 1120 g/kWh to 1130 g/kWh at E0 and E10 respectively. CO_2 then decreased to 1080 g/kWh at E100. Thermal efficiency increased from 22.5 % at E0 to 23.3 % at E100.
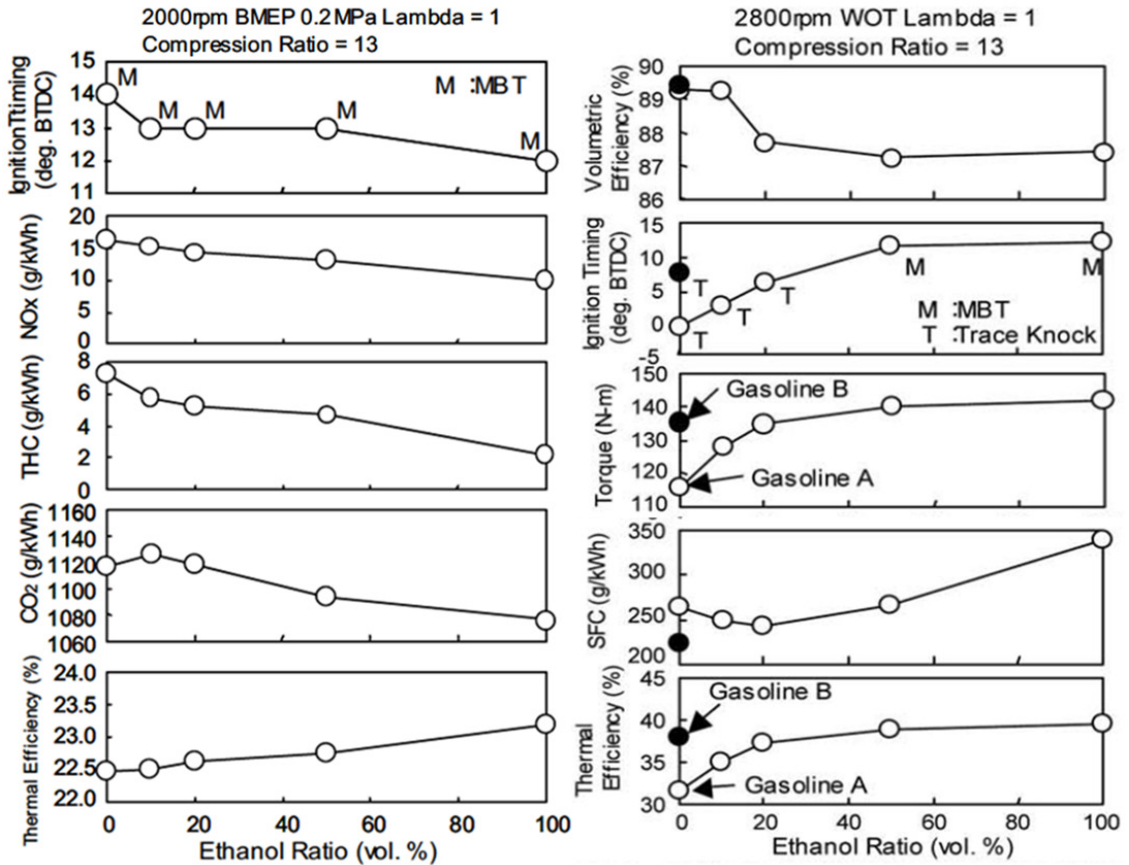
Figure 2.4[6]: Emissions and performance with different blends of ethanol utilizing a Toyota 1.5L engine.

Reprinted with permission from SAE Paper No. 2006-01-3380 © 2006 SAE International

2.2.4 Czerwinski et. al 2012, SAE 2010-01-0794

A decrease in CO was observed for all three scooters as ethanol content increased. CO emissions also decreased for hydrous ethanol when compared to the same concentration of anhydrous ethanol (Figure 2.5). This was expected due to the increasing oxygen content of the fuel as ethanol content increased. THC emissions decreased for the Kreidler and Honda. The Piaggio experienced an increase in THC emissions with rising ethanol content. This was attributed an increase in cyclic irregularities of combustion. Inversely with THC, NO_x emissions increased for the Kreidler and Honda while decreasing for the Piaggio.

Figure 2.5[7]: Emissions comparison of different blends of ethanol for three different scooters. The Honda is a four-stroke engine while the Piaggio and Kreidler are two-stroke engines.

Reprinted with permission from SAE Paper No. 2010-01-0794 © 2010 SAE International

2.3 Effects of Ethanol Blends on Engine Performance

Ethanol has a lower energy content by 39 % compared to gasoline. Due to the less complex fuel management systems of older vehicles and small engines, a reduction in power will be seen, as well as an increase in fuel consumption with adding ethanol to a base gasoline.

2.3.1 Ning et. al 2005, SAE 2005-32-0053

For this test maximum vehicle speed was used as a replacement for engine power. A reduction in maximum speed is assumed to correlate to a reduction in maximum power. Maximum speed decreased 2 % at 1,000 km and 5 % at 10,000 km. This is due

to the smaller heating value of ethanol compared to gasoline and the motorcycle's inability to adjust the air/fuel ratio to match that required by the E10 mixture. The larger decrease at 10,000 km compared to at 1,000 km also shows an increased degradation of the engine due to E10.

A constant speed of 25 km/h was used to determine fuel consumption with an ONOSOKI on board fuel flow meter. At 1,000 km, the fuel consumption was increased by 30 % and at 10,000 km the fuel consumption increased by 10%. The increase in fuel consumption is explained by the smaller heating value of ethanol compared to gasoline. One explanation of a smaller increase at 10,000 km than at 1,000 km is that the engines may not have been completely broken-in at 1,000 km. This would mean that frictional losses would be greater at 1,000 km than at 10,000 km. The frictional losses would require less gasoline than ethanol to balance the vehicle speed.

2.3.2 Nakata et. al 2006, SAE 2006-01-3380

The right column of Figure 2.4 shows thermal efficiency, BSFC, torque, ignition timing, and volumetric efficiency at 2800 rpm and WOT for different concentrations of ethanol. Volumetric efficiency decreased from 89 % to 87 % at E0 and E100 respectively with the largest difference between E10 and E20. Ignition timing was limited by knock until a concentration of 50 % ethanol was used. Engine torque increased from 117 Nm at E0 to 140 Nm at E100. The increase of torque was due to the advanced timing made possible by the increased octane number of ethanol. BSFC decreased from 260 g/kWh at E0 to 245 g/kWh at E20. The decrease in BSFC was due to a larger increase in power compared to the increase in fuel flow. BSFC increased at ethanol concentrations of 50 % and 100 % to 265 g/kWh and 340 g/kWh respectively. This increase in BSFC is due to the torque leveling off while fuel flow continued to increase. Thermal efficiency increased from 31 % to 40 % at E0 and E100 respectively.

2.3.3 Czerwinski et. al 2012, SAE 2010-01-0794

EGTs increased with increasing ethanol content for the Piaggio. The Kreidler saw an increase in EGT from E0 to E5 however EGTs decreased as ethanol concentration increased further. An initial decrease in EGT from E0 to E10 occurred on the Honda. EGTs then increased with increasing ethanol content. Maximum speed decreased for the Piaggio as ethanol concentration increased. The Kreidler's maximum speed decreased with ethanol content however with hydrous ethanol, maximum speed improved at and above EH10. An increase in maximum speed was observed for the Honda from E0 to E10. Maximum speed then decreased until E20 which had approximately the same maximum speed as E0.

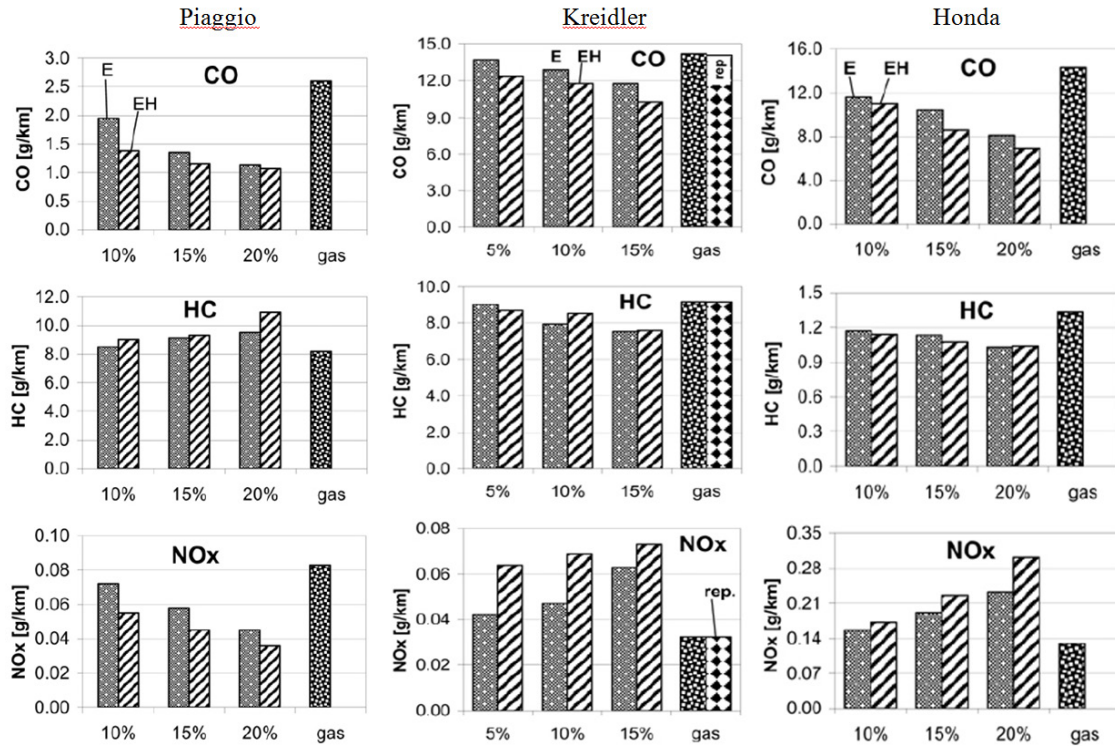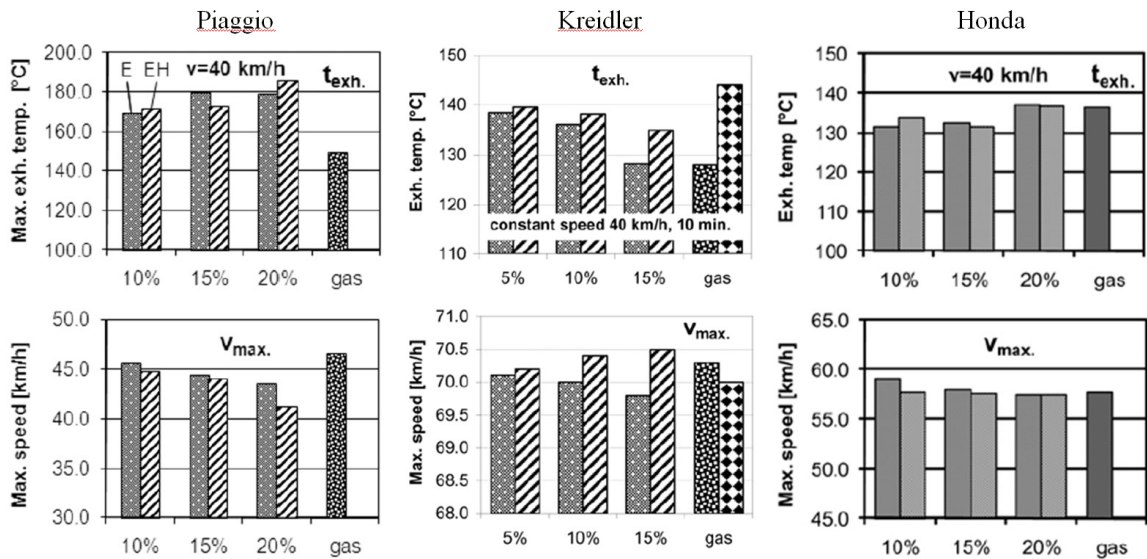**Figure 2.6[7]:** Engine performance comparison of different blends of ethanol for three different scooters. The Honda is a four-stroke engine while the Piaggio and Kreidler are two-stroke engines.

Reprinted with permission from SAE Paper No. 2010-01-0794 © 2010 SAE International

2.4 Literature Review Summary

In all four studies, THC decreased significantly with the addition of ethanol with the exception of the Piaggio scooter. The Piaggio scooter observed an increase in THC as ethanol content increased. This was due to poor engine performance and increased misfiring. In the first three tests, THC was reduced by nearly 20 % from E0 to E10. The second and third studies showed a further decrease of THC from E0 to E20 at about 25 %. The third study shows THC decreasing even further as ethanol concentration increases.

The motorcycles saw a 50 % decrease in CO from E0 to E10 while the automobiles in the second study only saw a decrease of 10 % to 15 %. This is probably due to the motorcycles carburetion whereas most of the automobiles had a closed-loop fuel injection system. The scooters also observed a significant decrease in CO.

There was a lot of variation in NOx emissions for the motorcycles. The NOx levels varied from a 30 % decrease to an 80 % increase. In the automobile test, the NOx tended to increase for the vehicles that did not apply LTFT and decrease for the vehicles that did apply LTFT. In the third test, NOx levels decreased as ethanol concentration was increased. This shows that engines that are adapted to ethanol can decrease NOx emissions while engines that cannot adapt tend to increase NOx. Due to the oxygen in ethanol, the engines that cannot adjust the air/fuel ratio for ethanol tend to run lean which increases combustion temperatures and available oxygen which in turn produces NOx.

The first two studies showed a 10 % increase in fuel consumption at E10 compared to E0. At E10, the third study found a 20 % decrease in specific fuel consumption. This is most likely due to the anti-knock quality of the ethanol. With ethanol, the ignition timing can be advanced which produces more torque and therefore power. The fuel consumption most likely increased slightly but because the fuel is still 90 % gasoline and therefore the overall heating value of the fuel does not drop significantly. This means that the slight increase in fuel consumption is smaller than the

increase in power which would drop specific fuel consumption. The power increase starts to level off at E20. At this point the fuel consumption continues to increase but the power has leveled off and therefore the BSFC starts to increase.

A decrease in power was observed in the motorcycles, while the third test saw an increase in power. This is due to two reasons. The first, being the motorcycles inability to decrease the air/fuel ratio for ethanol. This means that there is the same amount of fuel in the cylinder but the fuel mixture has less energy than straight gasoline. The motorcycles are also incapable of changing the timing to take advantage or ethanol's anti-knock quality. The engine in the third test, however, saw an increase in torque and therefore power. This is because the engine was able to adjust air/fuel ratio as well as ignition timing to improve power. The Piaggio and Kreidler scooters observed a decrease in maximum speed with increased ethanol content. The Kreidler, however, saw an increase in maximum speed with increasing hydrous ethanol concentration. The Honda observed an increase in maximum speed from E0 to E10. Maximum speed then decreased and leveled off with the same speed as E0.

Chapter 3 Experimental Setup

The purpose of this research was to determine the impact of E22 on two and four-stroke snowmobile emissions. Three snowmobiles were used for this testing and are shown in Table 3.2. These snowmobiles were chosen to represent a variety of current and available engine technologies. The picture of the Yamaha Apex is of a 2011 model however is representative of the snowmobile tested. The closed-loop fuel injection system of the Arctic Cat used feedback from an O_2 sensor to control relative air/fuel ratio. Relative air/fuel ratio was measured by comparing the partial pressure of O_2 in the exhaust to that of the ambient air. When excess O_2 was present in the exhaust, due to the enleanment effect of ethanol, fuel delivery was increased to maintain a consistent relative air/fuel ratio between the E0 and E22 fuels. To obtain the exhaust sample for the Yamaha and Polaris snowmobiles, a 0.25 inch stainless steel probe was inserted approximately 10 inches into the muffler. To obtain the exhaust sample for the Arctic Cat snowmobile, a 0.25 inch stainless steel probe was mounted in the exhaust pipe approximately 5 inches upstream of the muffler.

Emissions were taken on each of the snowmobiles with E0 and E22 utilizing a five mode test matrix. Each run of the five modes were repeated a total of three times. This was done to validate repeatability. An average of the three runs was then taken and a comparison was made between the two fuels. Fuel properties are shown in Table 3.1. Key differences of the E22 fuel are a reduced lower heating value and a numerically lower air/fuel ratio (AFR).

Table 3.1

Fuel properties of E0 and E22 used for testing.

Property	Unit	E0	E22
Lower Heating Value	MJ/kg	44	40.2
Stoichiometric AFR	-	14.58	13.34
RVP at 100° F	psi	10.98	12.33
Specific Gravity at 60° F	-	0.7527	0.763
Distillation, IBP	° F	88.5	87.6
Distillation, DP	° F	400.6	390.6
Ethanol Concentration	Vol %	0	21.4

Table 3.2

Snowmobiles and specifications used for testing.

Snowmobile	Engine	Fuel Injection System
2009 Arctic Cat Z1 Turbo Touring 8	Liquid Cooled, Turbo-Charged, Intercooled, 1056 cc, Two-Cylinder, Four-Stroke	Closed-Loop, Throttle Body Fuel Injection
2009 Yamaha Apex 9	Liquid Cooled, 998 cc, Four-Cylinder, Four-Stroke	Open-Loop, Port Fuel Injection
2010 Polaris Rush 10	Liquid Cooled, 599 cc, Two-Cylinder, Two-Stroke	Open-Loop, Semi-Direct Injection

3.1 Laboratory Test Setup

The following sections discuss the equipment and procedures used for this test. This includes the water brake dynamometer and engine cooling stand.

3.1.1 Water Brake Dynamometer Hardware

A Land and Sea water brake dynamometer (Figure 3.1), as well as, Land and Sea's DYNO-MAX software were used to control engine speed and load. The dynamometer was mounted directly to the taper of the crankshaft, the same way the primary clutch would be mounted for normal operation. A hall-effect sensor was used to acquire the engine speed. The torque arm was positioned over the jackshaft and with the use of a strain gauge, torque was obtained. Water flow and therefore load was controlled with the use of a stepper motor and load valve as seen in Figure 3.2. The throttle was controlled manually. The load valve was used to control engine speed. As the throttle was increased, water flow and therefore load would increase to maintain a constant engine speed. The throttle was then manipulated to maintain a certain engine torque.
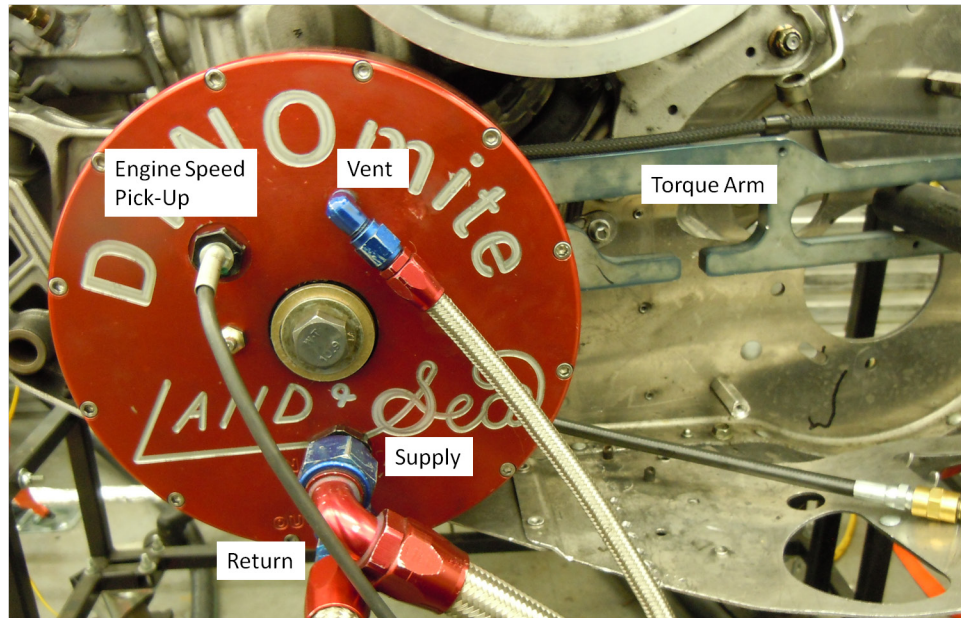
Figure 3.1: Land and Sea water brake dynamometer used to create load. The dynamometer is mounted on the crank of each snowmobile. The torque arm mounts on the jackshaft of each snowmobile.
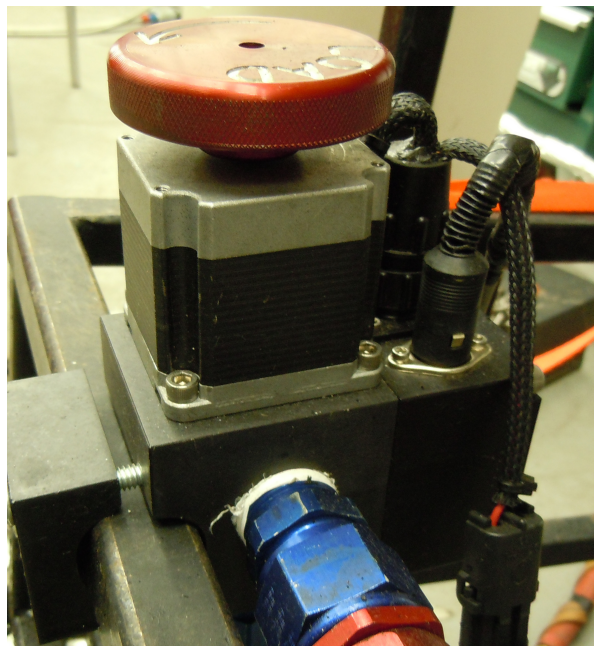
Figure 3.2: Dynamometer load control valve.

3.1.2 Engine Cooling Stand

To cool the engine, a cooling stand was built (Figure 3.3). A heavy duty radiator from a one-ton truck was used. A programmable two stage thermostat (Ranco ETC-211100-000) controlled a two speed, 24 inch Durafan, 7770 CFM fan to draw air across the radiator. On low the fan was capable of flowing 5825 CFM. These flows are based on a zero pressure drop. As shown in Figure 3.4, coolant was pumped from the radiator to a liquid to liquid heat exchanger. The snowmobile's cooling system was then connected to the liquid to liquid heat exchanger in a counter flow configuration. This kept the snowmobile's cooling system as close to production temperatures and pressures as possible.
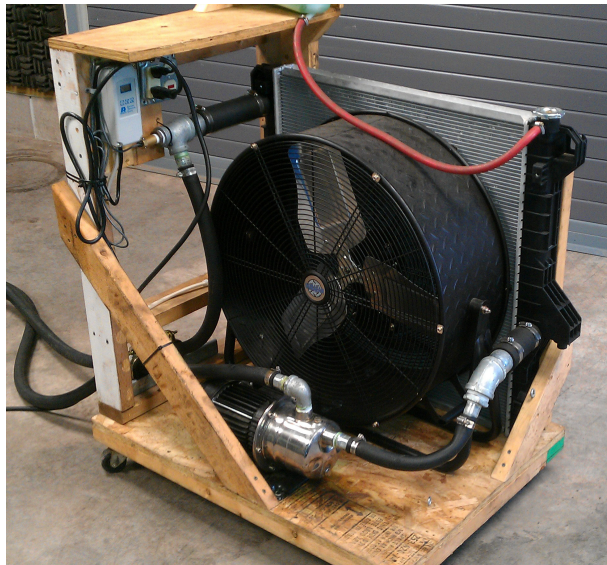
Figure 3.3: Engine cooling stand.
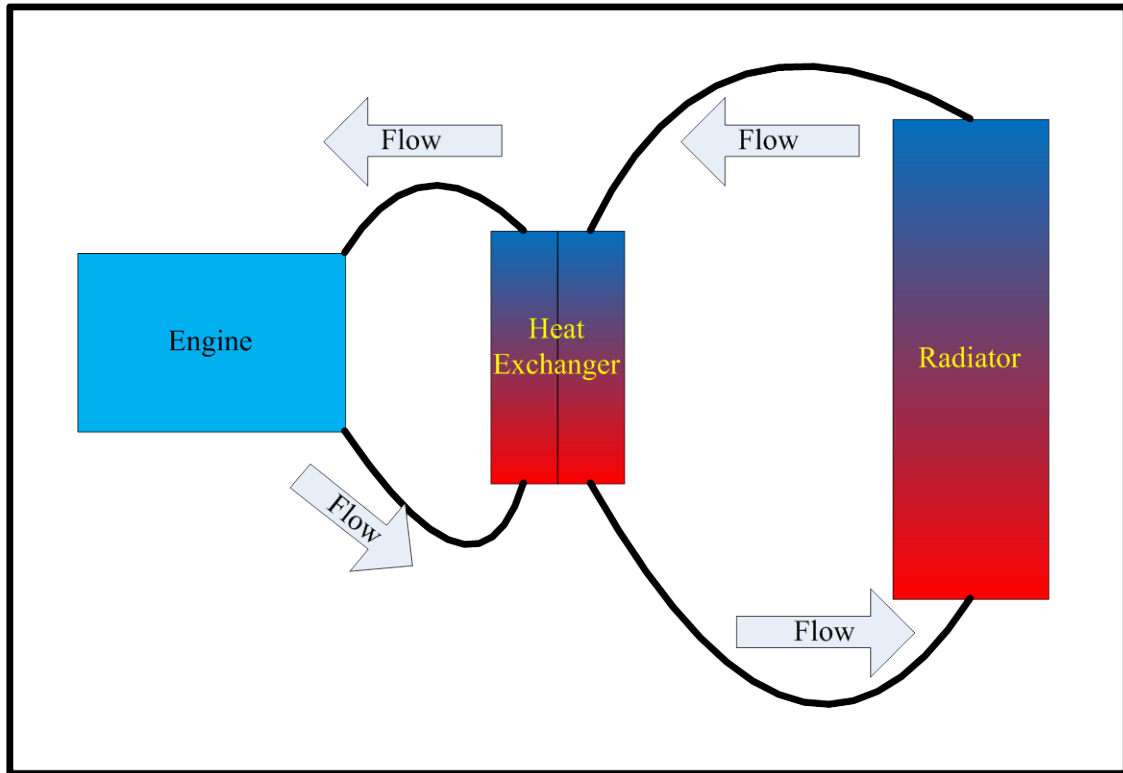
Figure 3.4: Coolant flow diagram. The heat exchanger was setup in a counter flow configuration.

3.2 Laboratory Instrumentation

The laboratory instrumentation consisted of DYNO-MAX software, Horiba emissions analyzer and AVL combustion analysis. DYNO-MAX was used to record engine parameters, such as: torque, engine speed and various temperatures. The Horiba emissions analyzer was used to record four emission gasses: total hydrocarbons (THC), carbon dioxide (CO_2), carbon monixide (CO), and diatomic oxygen (O_2). Combustion data was only taken on the Polaris snowmobile.

3.2.1 Dynamometer Software

DYNO-MAX by Land and Sea was used to record engine parameters. For better visibility in this thesis, the DYNO-MAX screen was divided into a left and right side screen shot (Figure 3.5 and Figure 3.6 respectively). Table 3.3 shows the engine

parameters recorded with DYNO-MAX. K-type thermocouples were used to measure temperatures. Some temperatures utilized varied from snowmobile to snowmobile. For instance, the number of exhaust gas temperatures (EGT(s)) depended on the number of cylinders of the snowmobile. Also, the Polaris was a two-stroke engine and therefore did not have an oil temperature. Power, air flow, brake specific fuel consumption (BSFC), fuel conversion efficiency and brake mean effective pressure (BMEP) were all calculated and the corresponding equation number is shown in the right column of Table 3.3. Data was recorded at 100 Hz and time averaged to 1 Hz.
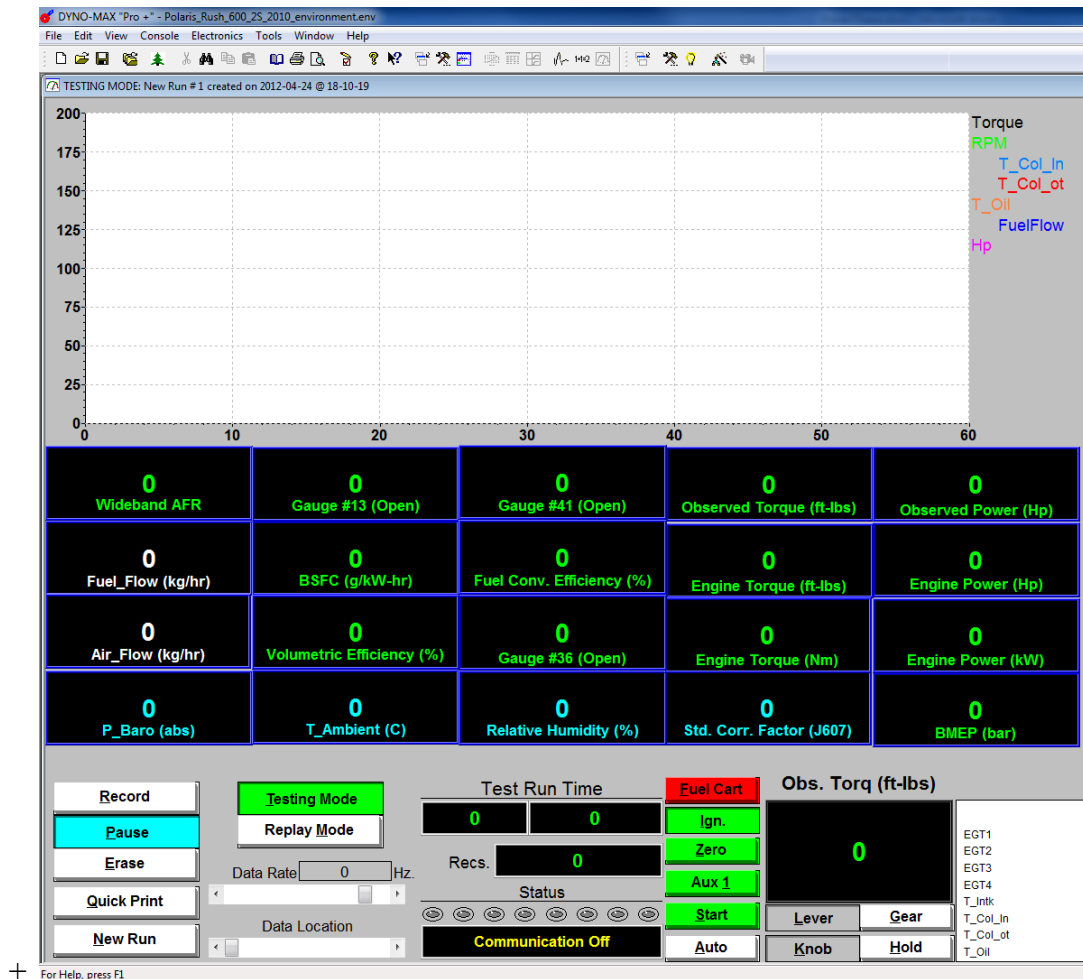
Figure 3.5: Left side of DYNO-MAX screen. The screen was cut in half for improved visibility in this thesis.
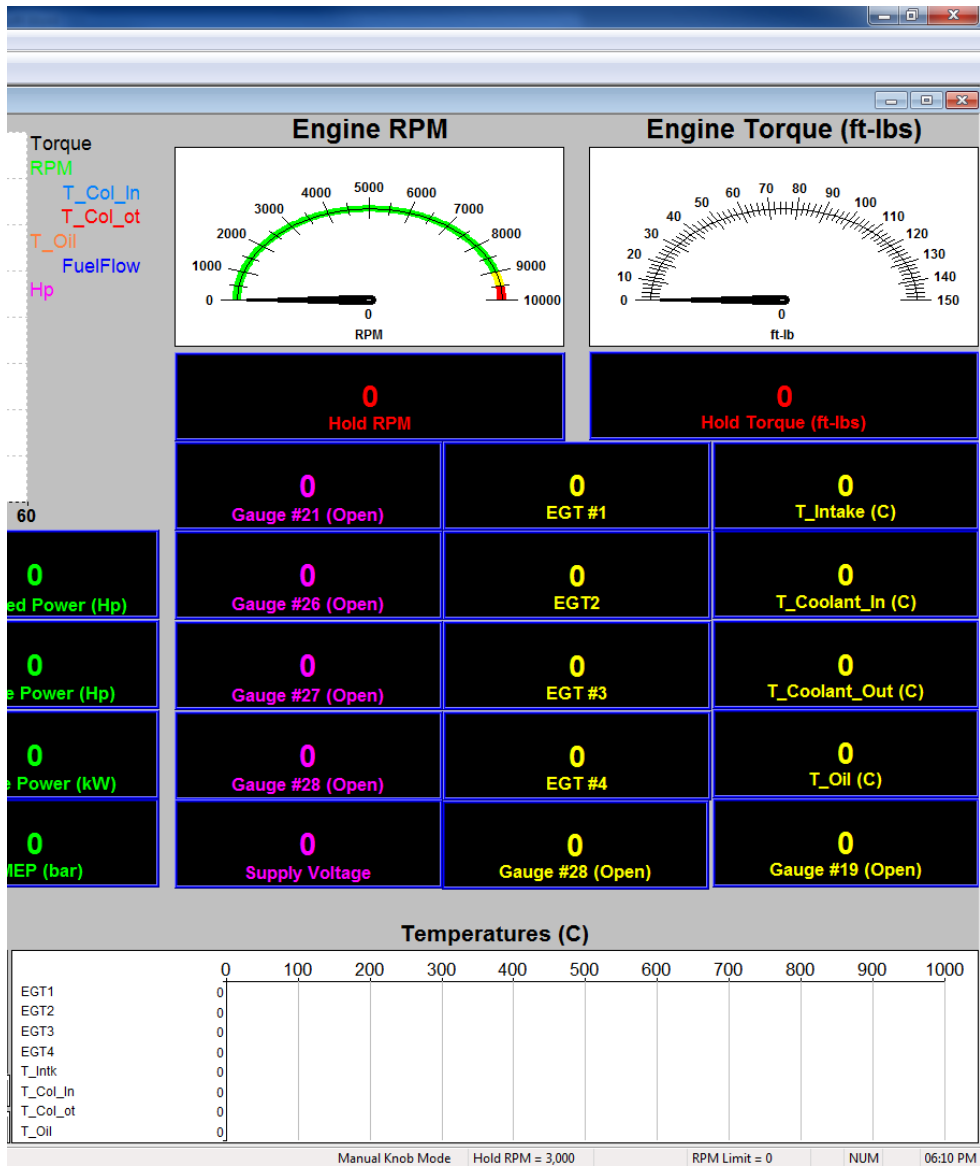
Figure 3.6: Right side of DYNO-MAX screen. The screen was cut in half for improved visibility in this thesis.

35

Table 3.3

Engine parameters recorded with DYNO-MAX.

Directly Measured		Calculated	
Temperatures (C)			**Equation**
Intake	Torque (ft-lb)	Power (horsepower)	*Eqn. 1*
Coolant In	Engine Speed (RPM)	Air Flow (kg/hr)	*Eqn. 2*
Coolant Out	Fuel Flow (kg/hr)	BSFC (g/kW-hr)	*Eqn. 3*
Oil	AFR (-)	BMEP (bar)	*Eqn. 4*
EGT(s)	Barometric Pressure (mbar)	Fuel Conversion Efficiency (%)	*Eqn. 5*
Ambient Air	Relative Humidity (%)		

$$P = \frac{N*T}{5252}$$ ....*Eqn. 1*

Where:

P is power in horsepower

N is engine speed in RPM

T is torque in ft-lb

$$\dot{m}_a = \dot{m}_f * AFR$$ ....*Eqn. 2*

Where:

$\dot{m}_a$ is mass air flow

$\dot{m}_f$ is mass fuel flow

$$BSFC = \frac{\dot{m}_f}{P(kW)} * \left[\frac{1000\ g}{1\ kg}\right]$$ ....*Eqn. 3*

$$BMEP = \frac{T*n_c*2*\pi}{V_d}..Eqn.\ 4$$

Where:

n_c is the number of revolutions per cycle

V_d is the displacement volume

$$\eta_f = \frac{P(kW)}{\dot{m}_f*LHV}..Eqn.\ 5$$

3.2.2 Emissions Analyzer

A Horiba MEXA 1600D five-gas emissions analyzer was used to obtain emissions data (Figure 3.7). The Horiba analyzer utilizes a non-dispersive infrared sensor (NDIR) to detect CO and CO_2 concentrations. THC concentrations are detected with the use of a flame ionization detector (FID). A chemoluminescence detector (CLD) is used for NOx detection and a magnetopneumatic detector (MPD) is used for O_2 detection. Table 3.4 shows the measurement range and repeatability for the various analyzers in the Horiba MEXA 1600D emissions analyzer.

Table 3.4

Measurement range and repeatability of Horiba analyzer.

Analyzer	Measurement Range	Repeatability
CO_2	0-16 Vol%	± 1 % of full scale
CO	0-10 Vol %	± 1 % of full scale
THC	0-50,000 ppmC1	± 1 % of full scale
O_2	0-25%Vol %	± 1 % of full scale

Figure 3.7: Horiba MEXA 1600D emissions analyzer.

3.2.3 Combustion Data Acquisition

Due to the faster flame speed of ethanol, a decrease in combustion duration, as well as, an advance in 50 % mass fraction burn was expected with the E22 fuel compared to the E0 fuel. AVL's IndiCom software and IndiModul 621 hardware were utilized to acquire crank angle and cylinder pressure. The AVL system is capable of a sampling rate up to 800 kHz per channel with a 14 bit ADC. An AVL 365C optical encoder was used to record crank angle position. The encoder had a resolution of 0.025 degrees. An AVL GU13Z-24 pressure transducer mounted in a custom spark plug adapter (Figure 3.8) was used to measure in-cylinder pressure. The GU13Z-24 pressure transducer had a sensitivity of 15.3 pC/bar. The in-cylinder pressure transducer data was utilized to

calculate indicated mean effective pressure (IMEP), combustion duration, and mass fraction burned (MFB).
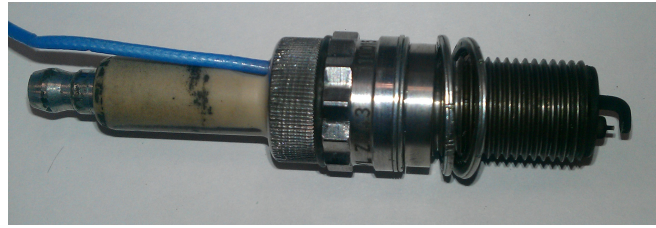
Figure 3.8: AVL GU13Z-24 pressure transducer mounted in custom spark plug adapter

3.2.4 Fuel Supply and Measurement Cart

The snowmobiles tested for this thesis all have fuel pumps in the fuel tank. The fuel is pressurized either at the pump or with a fuel pressure regulator located after the fuel rail. For the purpose of fuel flow measurement, the production fuel pump was disconnected and a Re-Sol fuel cart was used (Figure 3.8). The Re-Sol fuel cart contained a Coriolis flow meter which output a 4 mA to 20 mA signal depending on mass flow rate. A 250 Ohm resistor was used to convert the signal to a 1 V to 5 V signal which was then logged by DYNO-MAX. The fuel supply pressure was set to the manufacturer's fuel pressure for emission testing.
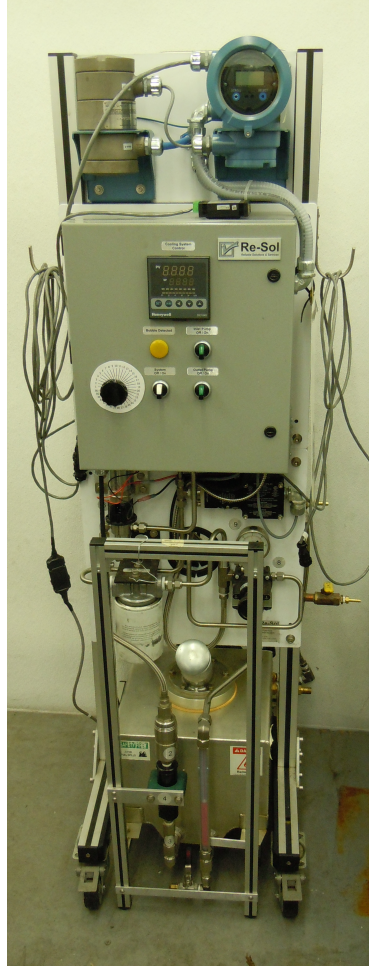
Figure 3.9: Re-Sol fuel flow cart.

3.2.5 O_2 Sensor and Mounting Hardware

    A NTK O_2 sensor was used on conjunction with a Powerdex AFX controller (Figure 3.9). For ease of installation and to prevent dilution, a tailpipe clamp mount from Pegasus Auto Racing Supplies was used (Figure 3.10).

Figure 3.10: Powerdex AFX controller used to monitor relative air/fuel ratio.

Figure 3.11: Tailpipe clamp mount used to mount the O_2 Sensor.

Chapter 4 Results

4.1 Test Matrix Description

Emissions were taken using the following test matrix. The test consisted of five steady state modes. Mode one is wide open throttle at peak power engine speed while mode five is idle. Modes two through four are a percentage of peak power engine speed and peak power torque. Table 4.1 shows the percentage of peak power engine speed and torque, as well as time for each mode. Due to climbing engine temperatures, mode one was limited to 1 minute where the rest of the modes were conducted for 2 minutes.

Peak power engine speed was found by conducting three power sweeps. The mean peak power engine speed was then used to determine each mode's engine speed. The engine was then held at mode one for 1 minute to determine a mean engine torque. The mean engine torque was then used to determine the other mode's engine torque.

The test started with E0 fuel. Mode one was completed first, followed by mode two and down to mode five. This was completed three times to ensure repeatability. The fuel cart was then flushed and filled with E22 fuel. Three runs of the five modes were then run with the E22 fuel.

Table 4.1

Test matrix.

Mode	Engine Speed (%)	Engine Torque (%)	Time (Minutes)
1	100	100	1
2	85	51	2
3	75	33	2
4	65	19	2
5	Idle	0	2

4.2 Wet to Dry THC Conversion

In order to calculate specific emissions, first dry THC must be calculated. This is done by calculating a correction factor (Eqn. 6). The correction factor is then multiplied by the wet concentration of THC to obtain the dry concentration.

$$K_w = 1 + \left[\frac{\alpha * \left[\frac{CO_{2\,dry}}{100} + \frac{CO_{dry}}{10^6} \right] + \left[\frac{2*P_v}{\phi*(P_b - P_v)} \right] * \left[\frac{CO_{2\,dry}}{100} + \frac{CO_{dry}}{10^6} + \frac{THC_{wet}}{10^6} \right] * \left[1 + \frac{\alpha}{4} - \frac{\beta}{2} \right]}{2 * \left[1 + \frac{\frac{CO_{dry}}{10^6}}{\frac{CO_{2\,dry}}{100} * 3.5} \right]} \right] \ldots\text{Eqn. 6}$$

Where:

K_w is the THC wet to dry correction factor

α is the atomic hydrogen/carbon ratio

β is the atomic oxygen/carbon ratio

$CO_{2\,dry}$ is the dry volume percent of CO_2

Φ is the dry equivalence ratio

P_v is the vapor pressure of water in kPa

P_b is the barometric pressure in kPa

THC_{wet} is the wet concentration of THC in ppmC1

4.3 Brake Specific Emissions Calculation

To convert from concentrations to brake specific emissions, equation 7 is used. Mode five brake specific emissions are not calculated. Mode five is at idle and therefore the power is zero. Brake power is in the denominator of equation 7 and therefore brake specific values cannot be calculated.

43

$$X_{BS} = \left[\frac{X_{dry}}{BP}\right] * \left[\frac{\dot{m}_f}{THC_{dry}*CO_{dry}*CO_{2\ dry}}\right] \left[\frac{MW_{air}}{MW_C+(\alpha*MW_H)+(\beta*MW_O)}\right]\ldots\ldots\ldots\ldots\text{Eqn. 7}$$

Where:

X_{BS} is the brake specific value of the desired pollutant in g/kW-hr

X_{dry} is the volume percent of the desired pollutant

BP is brake power in kW

$\dot{m}_f$ is the mass flow rate of fuel in g/hr

MW_{air} is the molecular weight of air

MW_C is the molecular weight of carbon

MW_H is the molecular weight of hydrogen

MW_O is the molecular weight of oxygen

4.4 Emissions Repeatability and Stability

To show the repeatability of the emissions data, the Yamaha Apex E0 CO_2 emissions are shown in the following figures (Figure 4.1 through Figure 4.5). It is important to note that the file for mode one run three was corrupted and therefore is not shown in the figures or used in the averages. Table 4.2 shows the standard deviation for each run as well as a combined standard deviation for each mode. The largest standard deviation occurred at mode three run three with a standard deviation of 0.151 %.

Table 4.2

Standard deviations of Yamaha CO_2 emissions.

Mode	Run 1	Run 2	Run 3	Combined
1	0.067	0.110	n/a	0.107
2	0.043	0.025	0.038	0.112
3	0.105	0.095	0.151	0.144
4	0.022	0.021	0.022	0.094
5	0.040	0.053	0.029	0.078
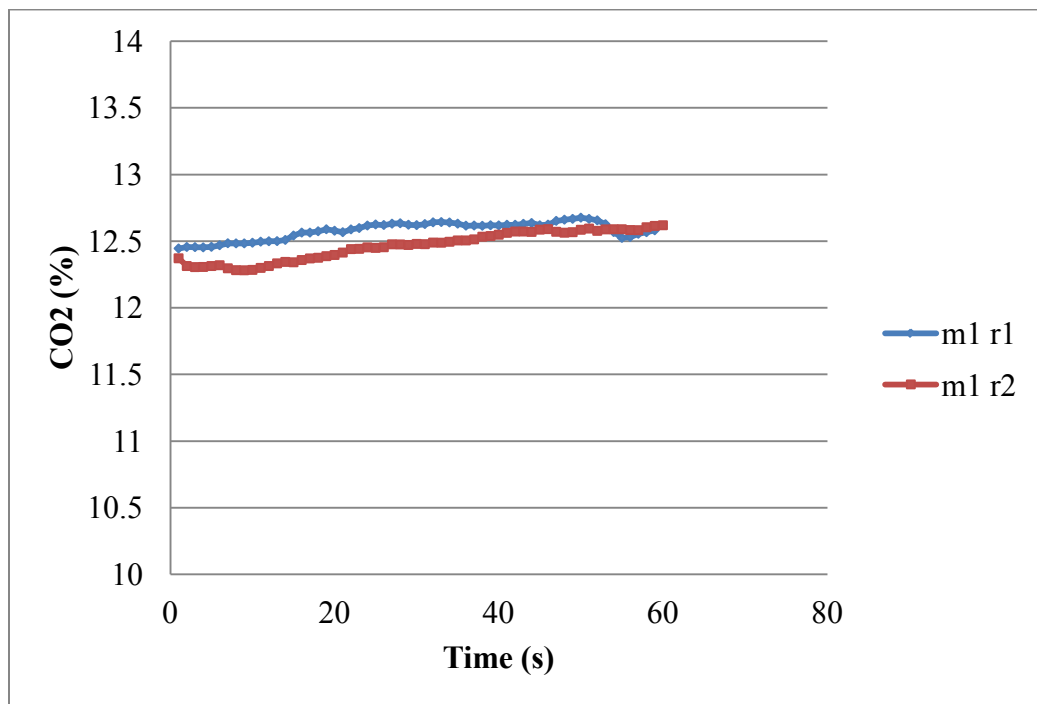
Figure 4.1: Mode one CO_2 emissions versus time.
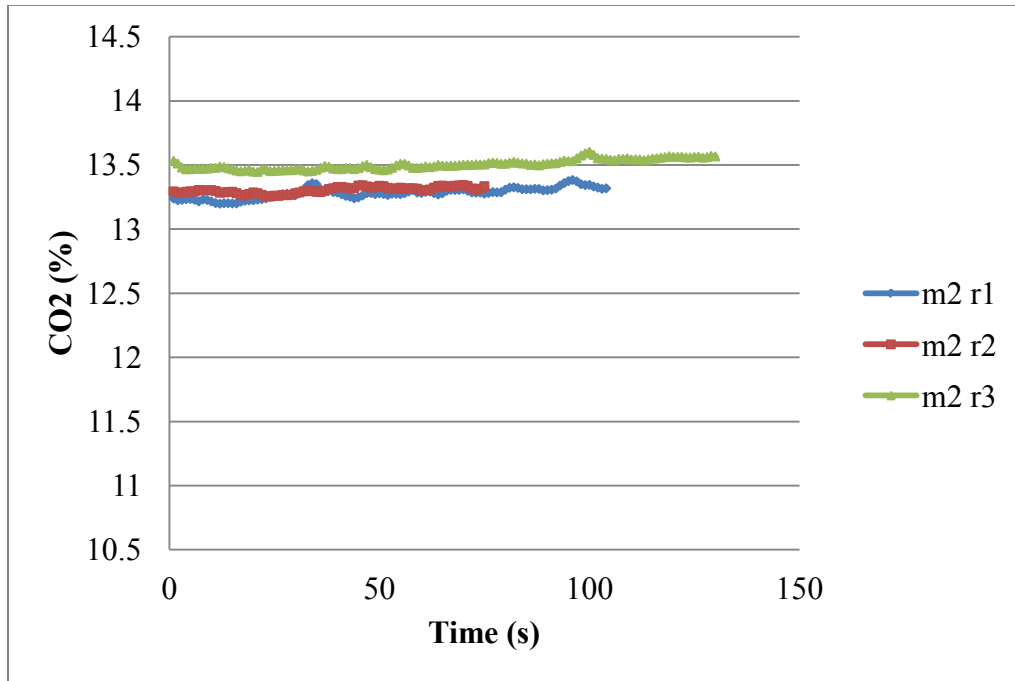
Figure 4.2: Mode two CO_2 emissions versus time.
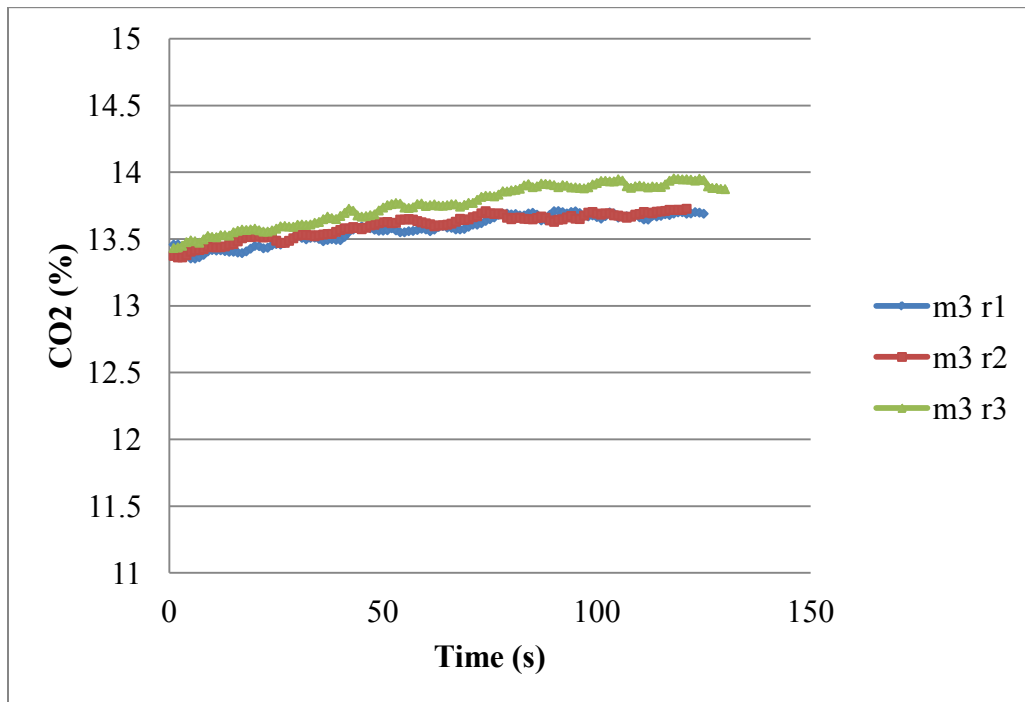
Figure 4.3: Mode three CO_2 emissions versus time.

46
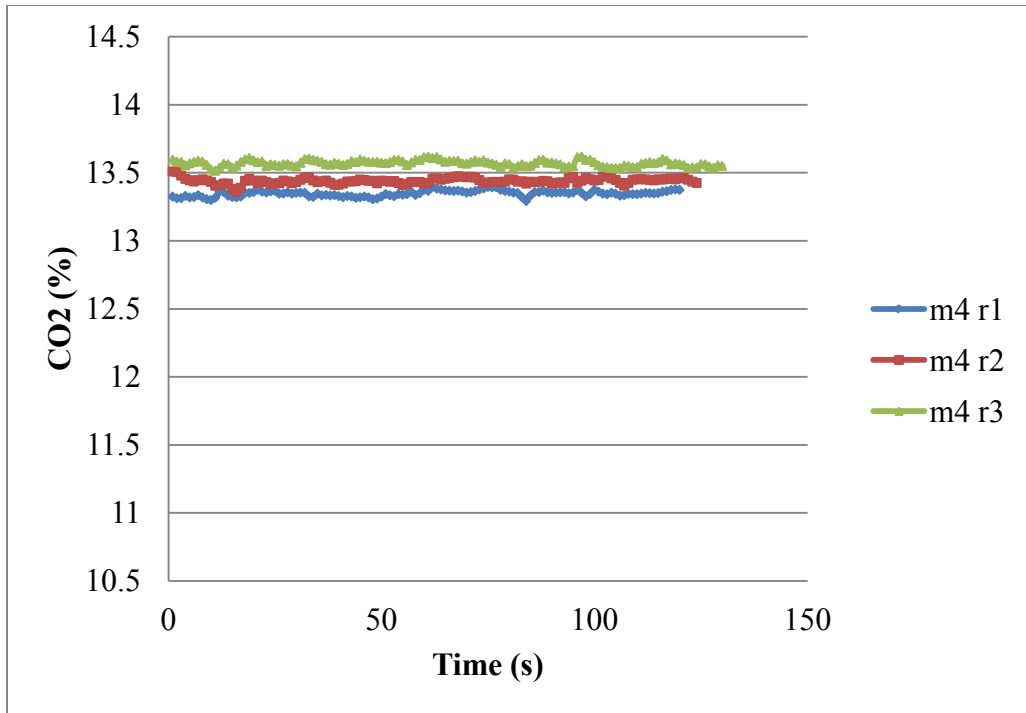
Figure 4.4: Mode four CO_2 emissions versus time.
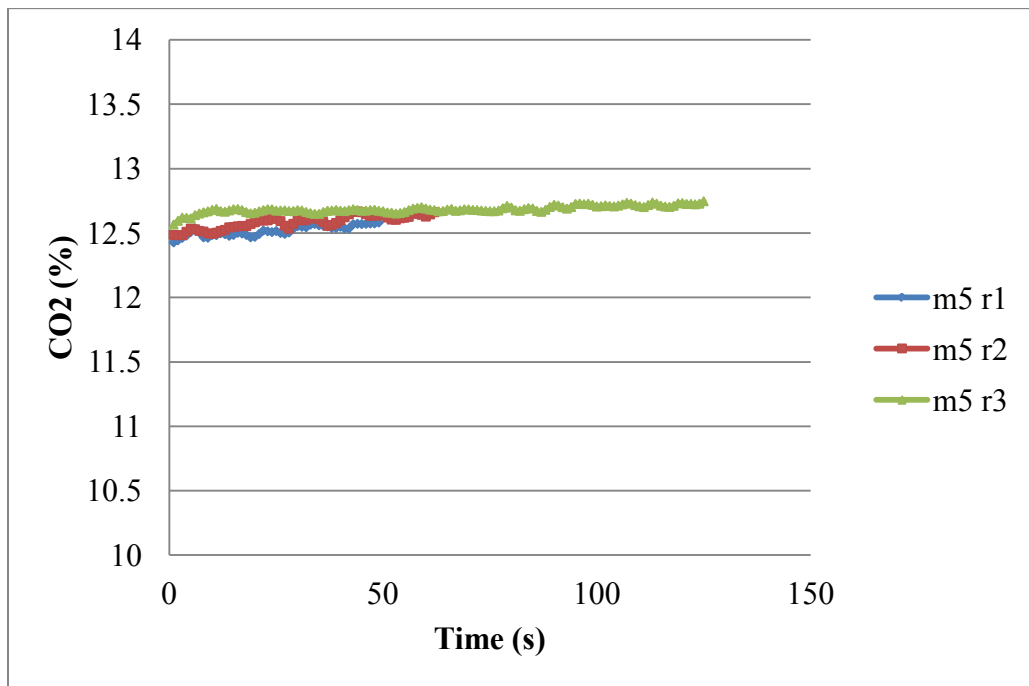
Figure 4.5: Mode five CO_2 emissions versus time.

4.5 E0 Emissions

4.5.1 Arctic Cat Z1 Turbo

Table 4.3 shows the averaged raw emissions of the five modes. The first and second run of E0 emissions contained negative O_2. For this reason, only O_2 from run three is shown instead of an average of the three runs. THC is shown in ppm on a C1 basis. Table 4.4 shows THC, CO, and CO_2 brake specific emissions in g/kW-hr.

Table 4.3

Raw E0 emissions for Arctic Cat.

Mode	THC (ppmC1)	CO Dry (%)	CO_2 Dry (%)	O_2 Dry (%)
1	6470	7.8	11.0	0.2
2	3484	4.4	12.9	0.3
3	1068	0.6	14.6	0.7
4	366	0.5	14.8	0.6
5	12867	7.3	11.0	0.7

Table 4.4

Brake specific E0 emissions for Arctic Cat.

Mode	THC (g/kW-hr)	CO (g/kW-hr)	CO_2 (g/kW-hr)
1	12.8	271.3	384.5
2	6.9	154.2	448.9
3	2.4	22.0	574.9
4	1.0	24.7	706.6

4.5.2 Yamaha Apex

Table 4.5 shows the averaged raw emissions for the Yamaha Apex. Run one had negative O_2 readings, therefore O_2 was averaged over runs two and three only. The emissions data file for mode one of run three was corrupted and therefore mode one emissions are averaged over runs one and two only. Table 4.6 shows the Yamaha brake specific emissions.

Table 4.5

Raw E0 emissions for Yamaha.

Mode	THC (ppmC1)	CO Dry (%)	CO_2 Dry (%)	O_2 Dry (%)
1	5750	4.7	12.5	0.8
2	6046	2.8	13.4	0.8
3	5101	2.3	13.7	0.7
4	3708	3.2	13.5	0.5
5	5784	4.8	12.6	0.8

Table 4.6

Brake specific E0 emissions for Yamaha.

Mode	THC (g/kW-hr)	CO (g/kW-hr)	CO_2 (g/kW-hr)
1	11.4	164.4	438.1
2	12.7	105.0	493.9
3	12.6	101.1	598.2
4	11.5	177.1	736.7

4.5.3 Polaris Rush

Table 4.7 shows the averaged raw emissions for the Polaris. Table 4.8 shows the brake specific emissions for the Polaris. Even though the Polaris is running rich of stoichiometric for modes one, two and four (Figure 4.24), the oxygen content is significantly higher than the four-stroke snowmobiles. The high oxygen content is due to the short circuiting of a two-stroke engine. Part of the intake charge escapes from the cylinder into the exhaust before the piston moves up high enough to block the exhaust port.

Table 4.7

Raw E0 emissions for Polaris.

Mode	THC (ppmC1)	CO Dry (%)	CO_2 Dry (%)	O_2 Dry (%)
1	20719	8.6	7.1	4.4
2	16013	3.8	10.4	4.2
3	14221	2.8	11.1	4.2
4	26965	6.1	8.9	4.6
5	46058	4.8	3.3	12.1

Table 4.8

Brake specific E0 emissions for Polaris.

Mode	THC (g/kW-hr)	CO (g/kW-hr)	CO_2 (g/kW-hr)
1	55.7	423.9	346.8
2	38.0	164.3	446.0
3	36.2	130.0	506.6
4	91.3	372.0	545.4

4.6 E22 Emissions and Comparison

4.6.1 Arctic Cat Z1 Turbo

The Arctic Cat had to be held at mode three for 2 minutes with E22 fuel before testing could be conducted. This allowed the fuel management system to learn the fuel and account for the higher ethanol concentration of E22. Table 4.9 shows the raw emissions for the Arctic Cat using E22 as a fuel. Modes two and three contained negative O_2 and have been omitted from the raw emissions shown. Table 4.10 shows the brake specific emissions while running on E22.

Table 4.9

Raw E22 emissions for Arctic Cat.

Mode	THC (ppmC1)	CO Dry (%)	CO_2 Dry (%)	O_2 Dry (%)
1	4490	7.2	11.0	0.1
2	2317	3.5	13.0	0.2
3	766	0.5	14.4	0.5
4	248	0.5	14.5	0.5
5	8441	4.5	12.1	0.5

Table 4.10

Brake specific emissions for Arctic Cat.

Mode	THC (g/kW-hr)	CO (g/kW-hr)	CO_2 (g/kW-hr)
1	9.2	262.1	402.7
2	4.8	129.6	481.0
3	1.8	20.7	583.9
4	0.7	25.0	738.7

Table 4.11

Percent change in brake specific emissions for Arctic Cat.

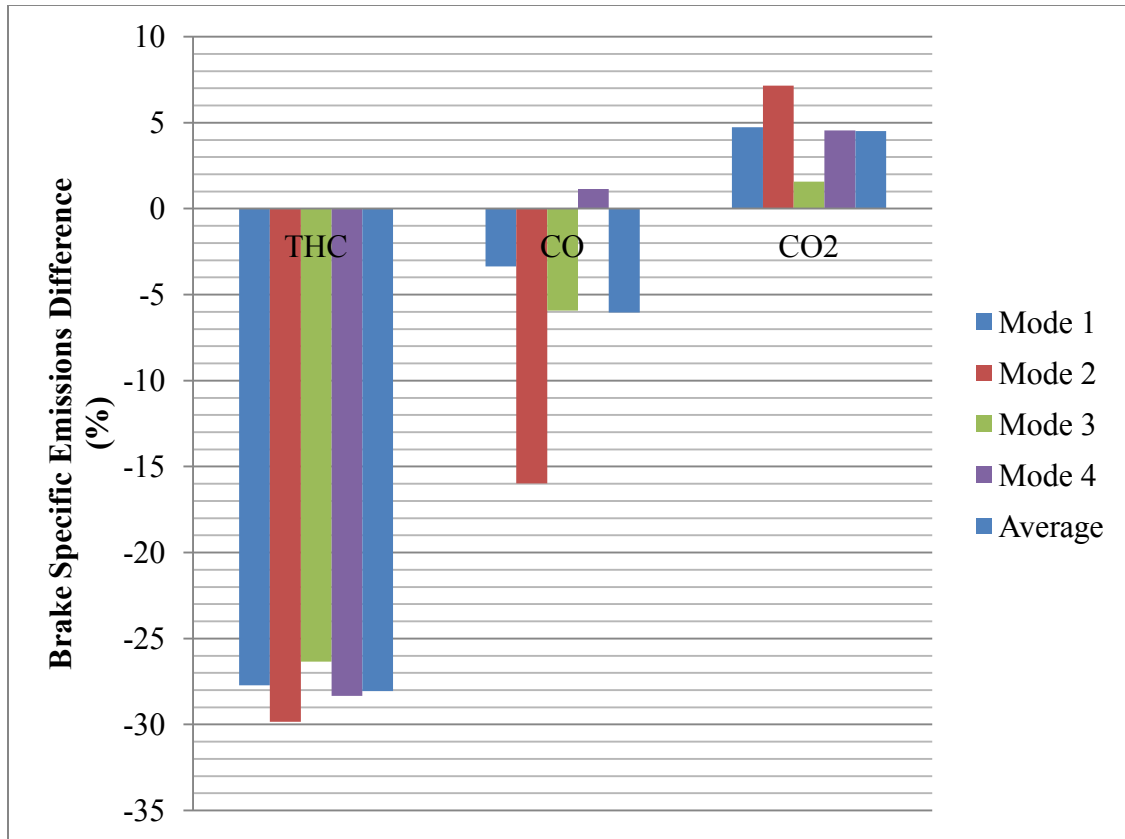| Mode	THC (%)	CO (%)	CO_2 (%)
1	-27.7	-3.4	4.7
2	-29.8	-16.0	7.2
3	-26.3	-5.9	1.6
4	-28.3	1.2	4.5
Average	-28.0	-6.0	4.5

Figure 4.6: Difference in brake specific emissions from E0 to E22 for the Arctic Cat.

Table 4.11 shows the percent change in brake specific emissions from E0 to E22. THC dropped for all modes by an average of 28 %. CO dropped for all modes except for mode four which increased by 1.2 %. The average decrease of CO was still 6 %. CO_2 increased on average by 4.5 % for modes one through four. When compared to the other snowmobile engines, the change in brake specific emissions, due to the change in fuel, was much smaller. This is due to the closed-loop fuel injection system. The engine was able to maintain the same relative air/fuel ratio and therefore did not operate lower than the factory calibration.

4.6.2 Yamaha Apex

Table 4.12 shows the raw emissions for the Yamaha with E22 for fuel. Table 4.13 shows the brake specific emissions.

Table 4.12

Raw E22 emissions for Yamaha.

Mode	THC (ppmC1)	CO Dry (%)	CO_2 Dry (%)	O_2 Dry (%)
1	3531	1.6	13.8	0.8
2	3369	0.9	13.8	1.4
3	2687	0.3	13.9	1.7
4	1522	0.6	14.4	0.7
5	2532	1.6	14.0	0.6

Table 4.13

Brake specific E22 emissions for Yamaha.

Mode	THC (g/kW-hr)	CO (g/kW-hr)	CO_2 (g/kW-hr)
1	7.8	61.4	538.2
2	7.9	37.6	576.9
3	7.7	17.8	708.5
4	5.5	37.9	902.5

Table 4.14 shows the percent change in brake specific emissions for the Yamaha with E22. THC decreased on average by 40 %. CO decreased on average by 72 %. CO_2 increased by 20 %. The Yamaha fuel injection system was open-loop. This means that the same amount of fuel was injected for E0 and E22 thus the E22 combustion was leaner than that of E0. The increase in oxygen due to leaner combustion contributes to the increase of CO_2 and decrease of CO and THC.

Table 4.14

Percent change in brake specific emissions for Yamaha.

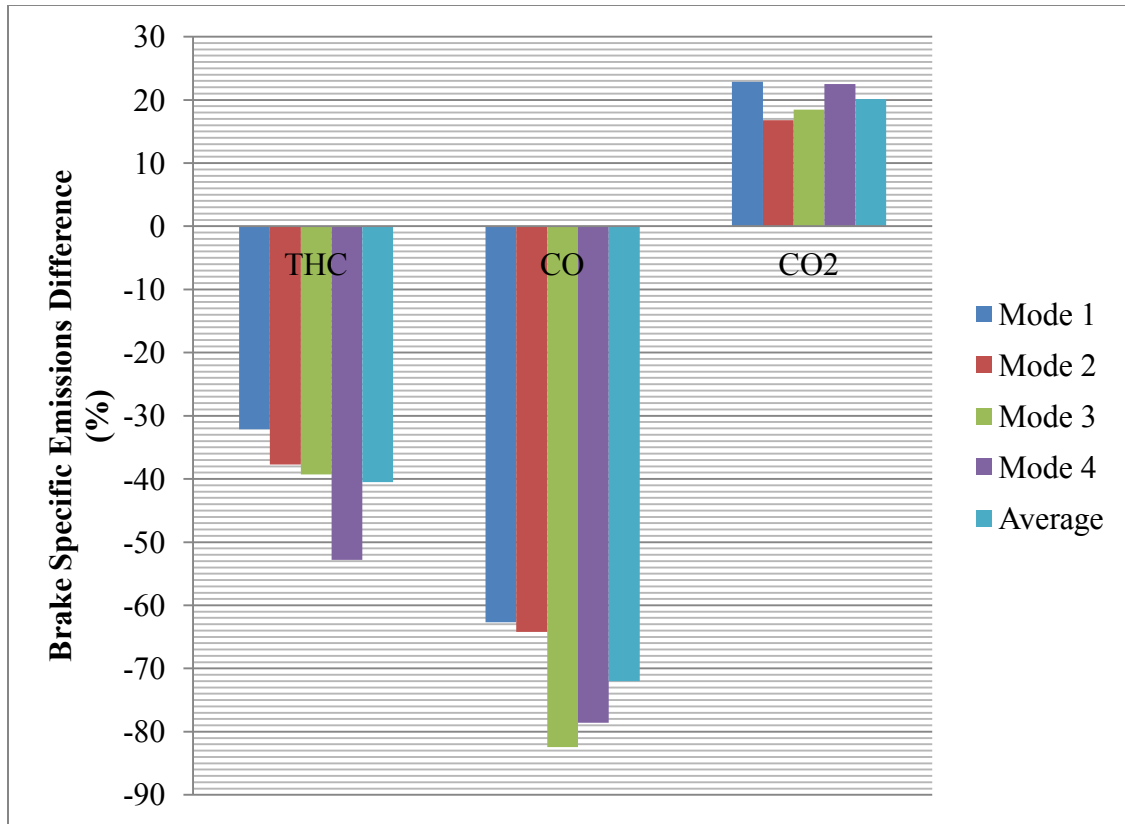| Mode	THC (%)	CO (%)	CO_2 (%)
1	-32.1	-62.7	22.8
2	-37.7	-64.2	16.8
3	-39.3	-82.4	18.5
4	-52.8	-78.6	22.5
Average	-40.5	-72.0	20.2

Figure 4.7: Difference in brake specific emissions from E0 to E22 for the Yamaha.

4.6.3 Polaris Rush

The Polaris had a resistor that could be changed for different concentrations of ethanol. This allowed the fuel management system to change control parameters to account for the ethanol. The only resistor options were E0 and E10. The E10 resistor was used for testing the E22 fuel. The fuel management system was therefore only partially able to account for the higher ethanol concentration of E22. Table 4.15 shows the raw emissions for the Polaris running on E22. Table 4.16 shows the brake specific emissions for the Polaris running on E22. The engine speed for mode four of run three was set to the wrong speed and this data was omitted from the averages.

Table 4.15

Raw E22 emissions for Polaris.

Mode	THC (ppmC1)	CO Dry (%)	CO_2 Dry (%)	O_2 Dry (%)
1	17897	7.7	7.4	4.1
2	11607	3.4	10.7	3.6
3	9602	1.7	11.3	4.4
4	25511	2.7	10.5	4.8
5	46136	4.7	3.9	11.5

Table 4.16

Brake specific E22 emissions for Polaris.

Mode	THC (g/kW-hr)	CO (g/kW-hr)	CO_2 (g/kW-hr)
1	52.4	412.4	394.4
2	29.9	156.9	498.1
3	26.7	85.4	569.5
4	89.4	173.1	665.2

Table 4.17 shows the percent change in brake specific emissions. THC decreased for all four modes. On average, THC decreased by 13.9 %. CO decreased by 23.8 % on average with a larger decrease at modes three and four. A smaller decrease was observed for modes one and two. CO_2 increased on average by 14.9 %.

Table 4.17

Percent change in brake specific emissions for Polaris.

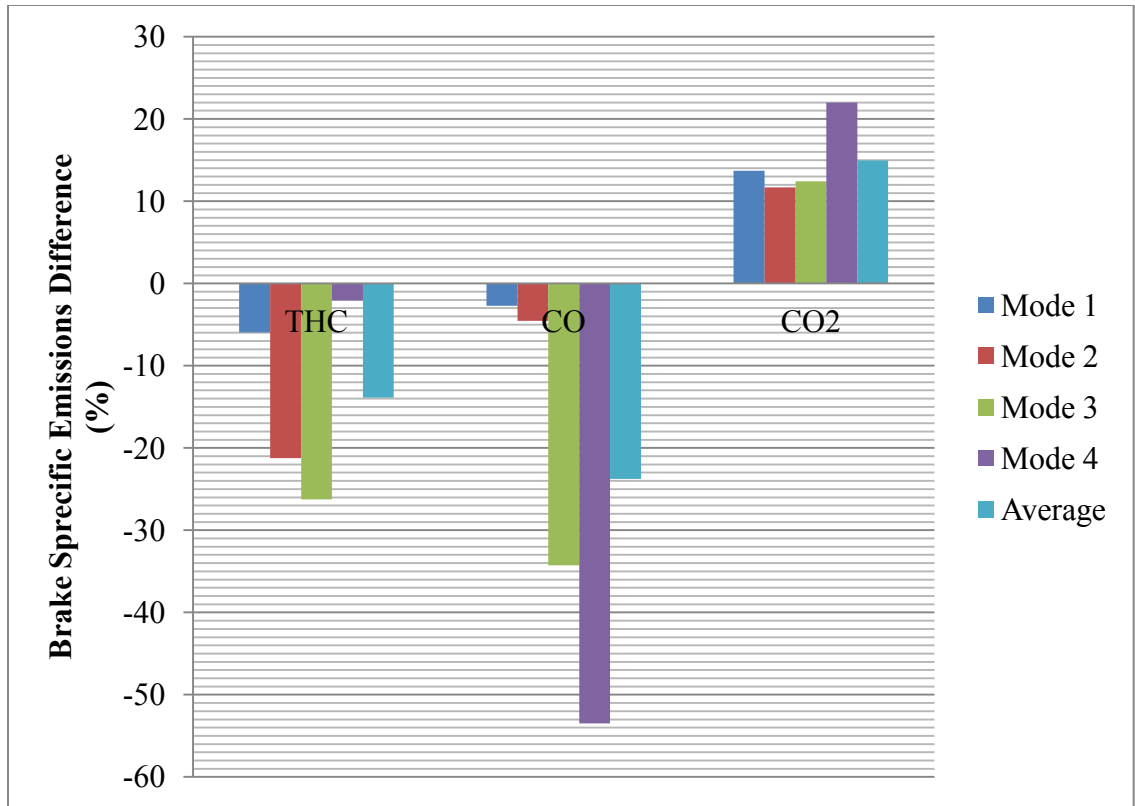| Mode	THC (%)	CO (%)	CO_2 (%)
1	-5.9	-2.7	13.7
2	-21.2	-4.5	11.7
3	-26.2	-34.3	12.4
4	-2.1	-53.5	22.0
Average	-13.9	-23.8	14.9

Figure 4.8: Difference in brake specific emissions from E0 to E22 for the Polaris.

4.6.4 Emissions Comparison Summary

To summarize the effect of E22 on emissions they were averaged over all modes for each snowmobile. The average for the E0 fuel was then subtracted from the average of the E22 fuel. This averaging shows a net effect of E22 on emissions. Figure 4.9 shows the average change in brake specific THC emissions. The smallest change was observed with the closed-loop fuel injected Arctic Cat with a 1.6 g/kW-hr decrease. All three snowmobiles observed an average decrease in brake specific THC emissions for the E22 fuel compared to the E0 fuel.
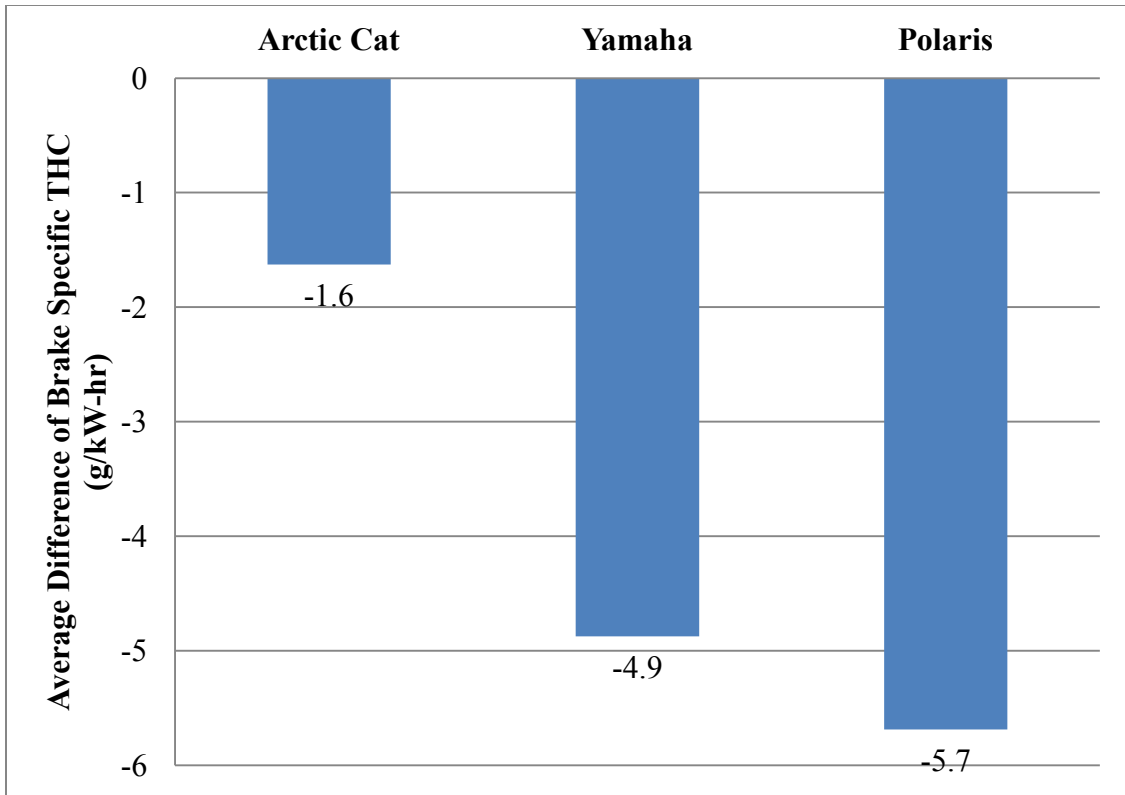
Figure 4.9: Average difference in brake specific THC.

Figure 4.10 shows an average decrease in brake specific CO emissions for all three snowmobiles. The closed-loop fuel injected Arctic Cat had the smallest decrease in brake specific CO emissions with an 8.7 g/kW-hr decrease from E0 to E22. The largest decrease was observed with the open-loop Yamaha with a 98.2 g/kW-hr decrease.
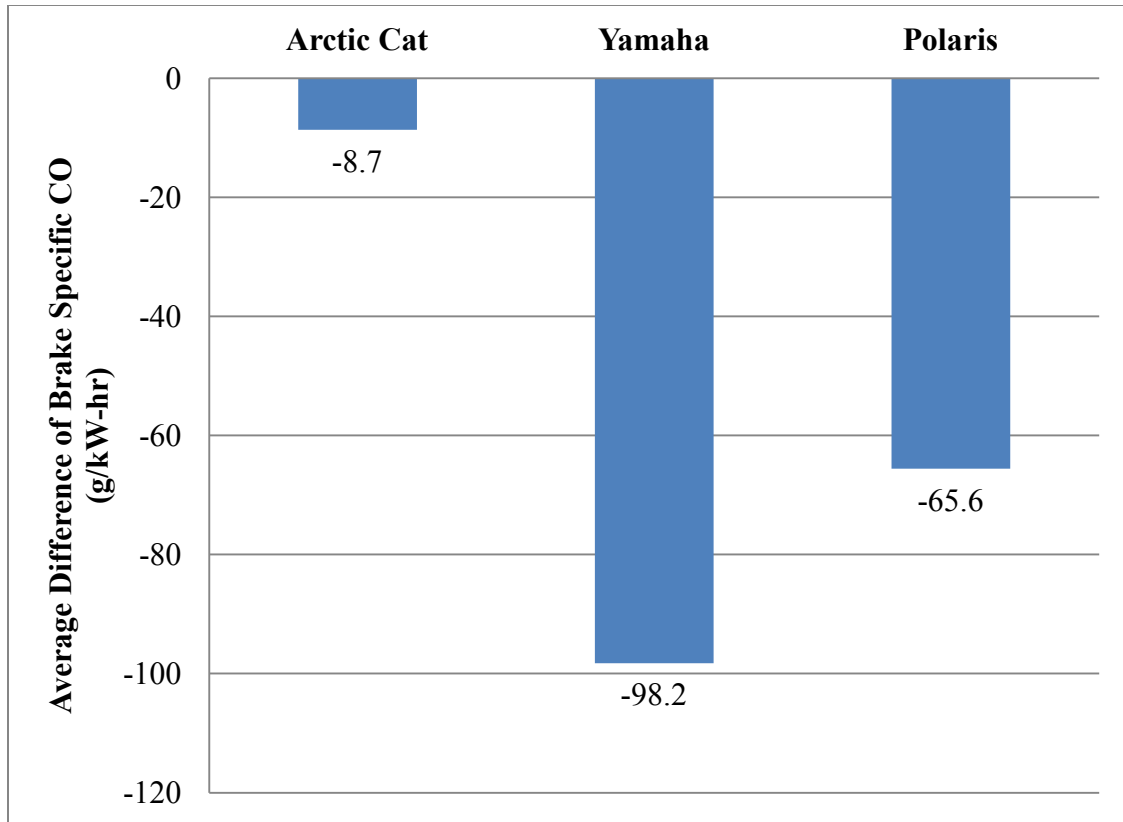
Figure 4.10: Average difference in brake specific CO emissions.

Figure 4.11 shows an average increase in brake specific CO_2 emissions for all three snowmobiles. An increase in CO_2 emissions was expected due to the decrease in CO emissions. The smallest increase was observed with the closed-loop Arctic Cat with an increase of 22.9 g/kW-hr.
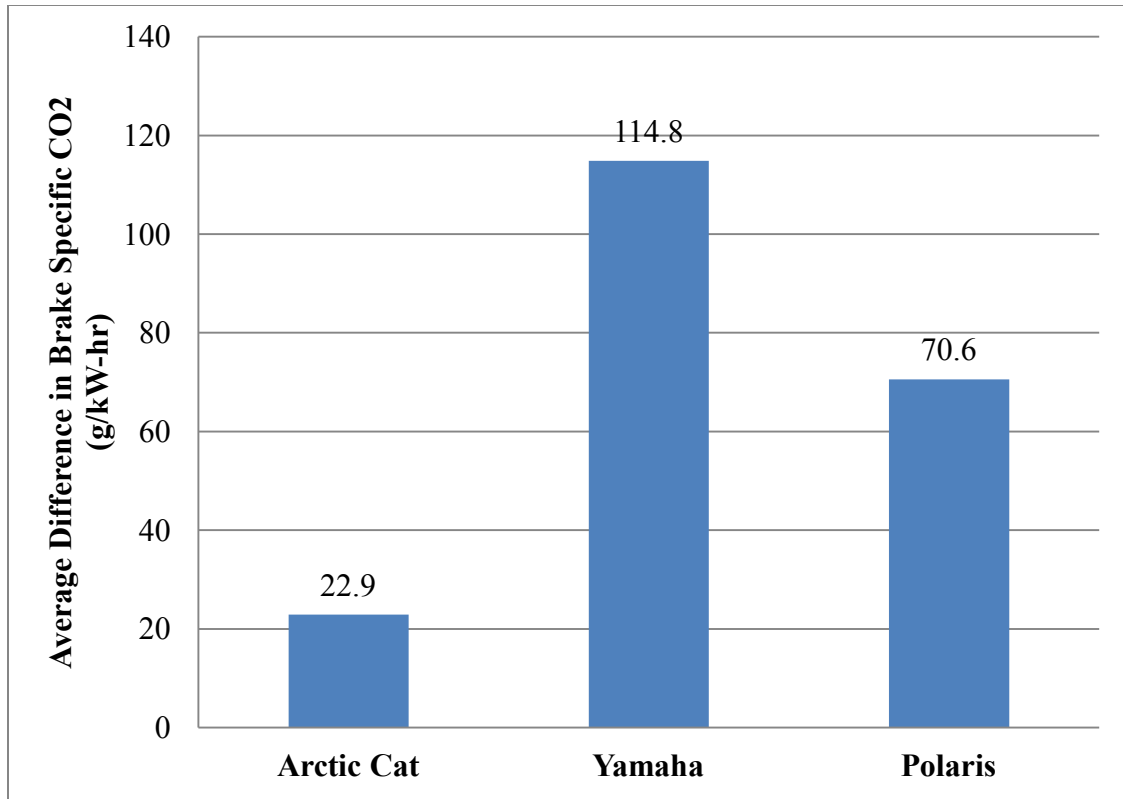
Figure 4.11: Average difference in brake specific CO_2 emissions.

4.7 Peak Power Comparison

The Arctic Cat, due to closed-loop fuel injection, had the largest increase of peak power at 2.4 % (Table 4.18). This is attributed to the oxygen content of the ethanol. The oxygen content of the fuel forced the fuel management system to inject more fuel to overcome the change in stoichiometric AFR. A 1.4% increase in power was observed with the Polaris. The increase of power for Polaris was due to the E10 resistor. The fuel management system injected more fuel to account for the change of stoichiometric AFR of E10. The change of stoichiometric AFR from E0 to E10 is 47 % of the change from E0 to E22, thus the fuel management system only partially adapted to the change in stoichiometric AFR. The Yamaha had no means to account for increased ethanol content in the E22 fuel. This means that the same amount of fuel was injected regardless of

ethanol concentration as a result, a 1.6 % decrease in power is the result of the decreased heating value

Table 4.18

Comparison of peak observed powers.

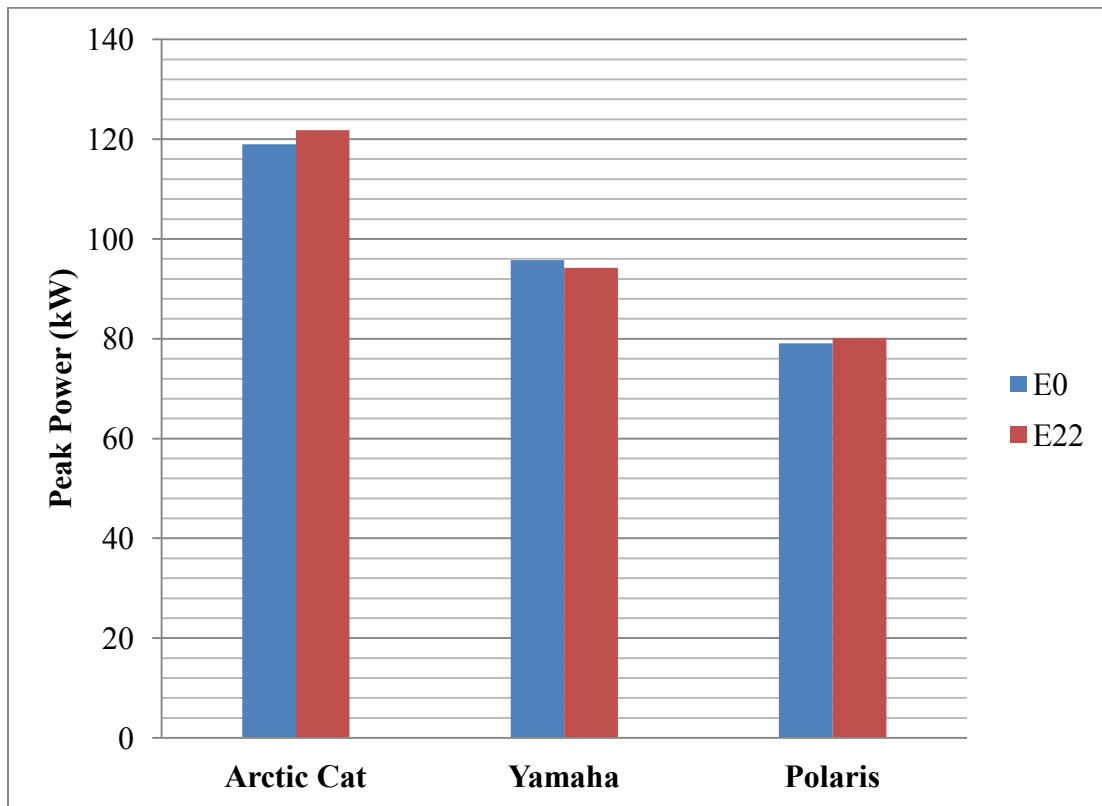| Snowmobile	Peak Power E0 (kW)	Peak Power E22 (kW)	Percent Difference (%)
Arctic Cat	119.0	121.8	2.4
Yamaha	95.8	94.2	-1.6
Polaris	79.1	80.2	1.4

Figure 4.12: Comparison of peak observed powers.

4.8 Engine Performance Comparison

The engine parameters discussed within this section are: an average of the exhaust gas temperatures, fuel flow, BSFC, and relative air/fuel ratio (λ). Due to problems with fresh air dilution with the NTK O_2 sensor, λ was calculated using the Horiba emissions analyzer.

4.8.1 Arctic Cat Z1 Turbo

Figure 4.10 shows the power at each mode for the Arctic Cat for both fuels. Modes two through four were held at the same torque and engine speed for each fuel and therefore there should be no difference between E0 and E22. The differences observed were due to the limits of repeatability of the manual throttle and the engine speed control. Mode one is at WOT and torque was allowed to vary between the two fuels.
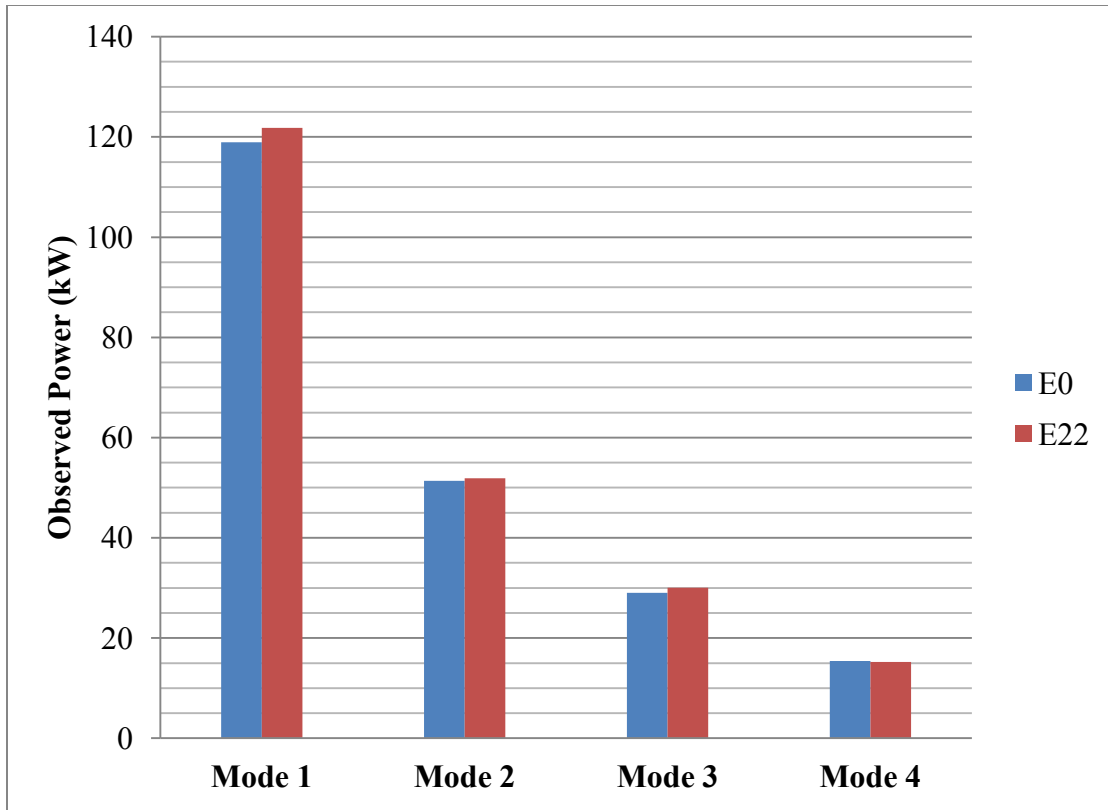
Figure 4.13: Comparison of power at each mode for the Arctic Cat. Power at each mode should be identical for E0 and E22 for modes two through four.

Only one exhaust gas temperature was recorded for the Arctic Cat at the inlet to the turbine and therefore only the average of that exhaust gas temperature is shown. Figure 4.11 shows the average exhaust gas temperatures for the five modes of E0 and E22. EGTs decreased for E22 for every mode except mode five. A 2° C increase was observed for mode five. The decrease in exhaust gas temperature with E22 was due to charge cooling caused by the increased latent heat of vaporization of ethanol and the ability of the closed-loop fuel injection system to maintain λ. This is verified by an increase in fuel flow shown in Figure 4.12. On average, exhaust gas temperatures dropped by 17.6° C.
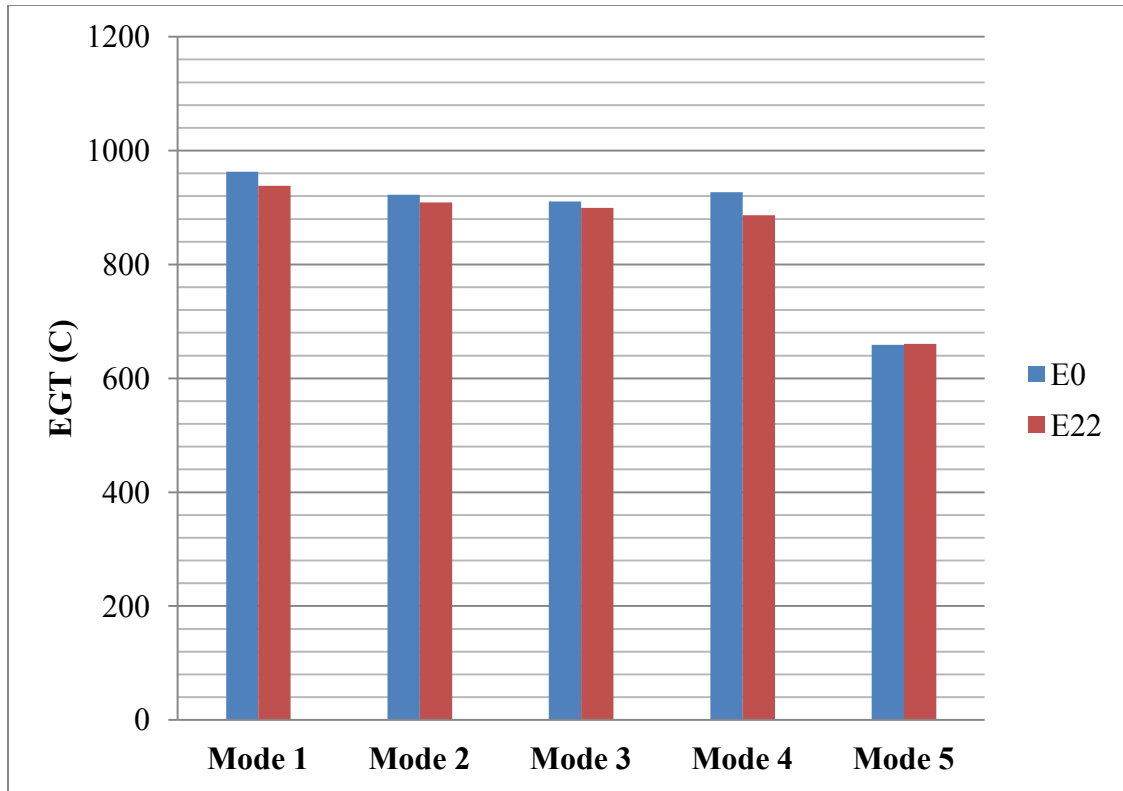
Figure 4.14: Comparison of Arctic Cat exhaust gas temperature.

Figure 4.12 shows the fuel flow for the five modes of each fuel. Fuel flow increased for each mode with the exception of mode five. Fuel flow for mode five decreased by 0.07 kg/hr, which is a 6.2% decrease. The increase in fuel flow is due to the closed-loop fuel injection. In order to maintain λ for the E22 fuel, the fuel management system was forced to inject more fuel causing the fuel flow to increase.
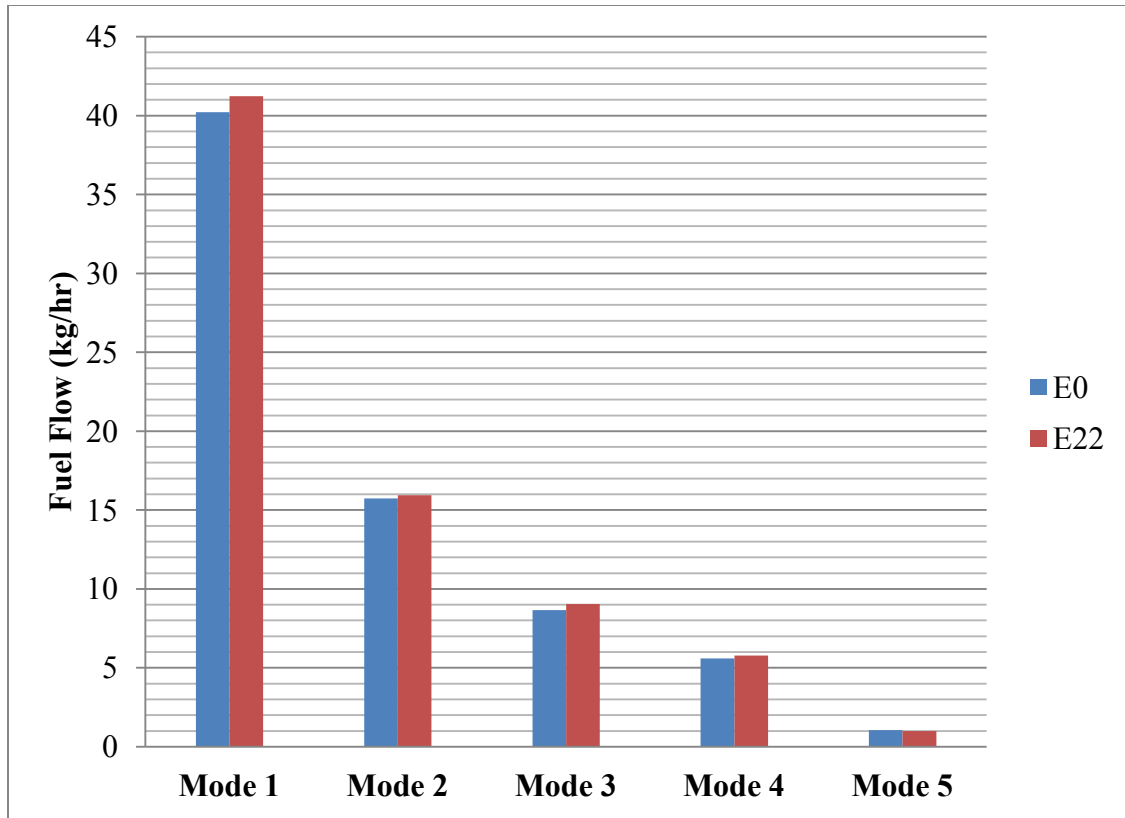
Figure 4.15: Comparison of Arctic Cat fuel flow.

To normalize fuel flow differences, Figure 4.13 shows the BSFC comparison for modes one through four. A BSFC increase of less than 1 % was observed for modes one, two and three. Peak power (mode one) increased by 2 % while fuel flow increased by 2.5 % (Table 4.19). As seen in Equation 3, if power and fuel flow increase by the same percentage then BSFC will remain the same. In the case of mode one, fuel flow increased slightly more than power and therefore a slight increase in BSFC was observed. In the case of mode four, power decreased by 1.9 % and fuel flow increased by 3.1 %. The decrease of power and increase of fuel flow resulted in a 4.4 % increase in BSFC.
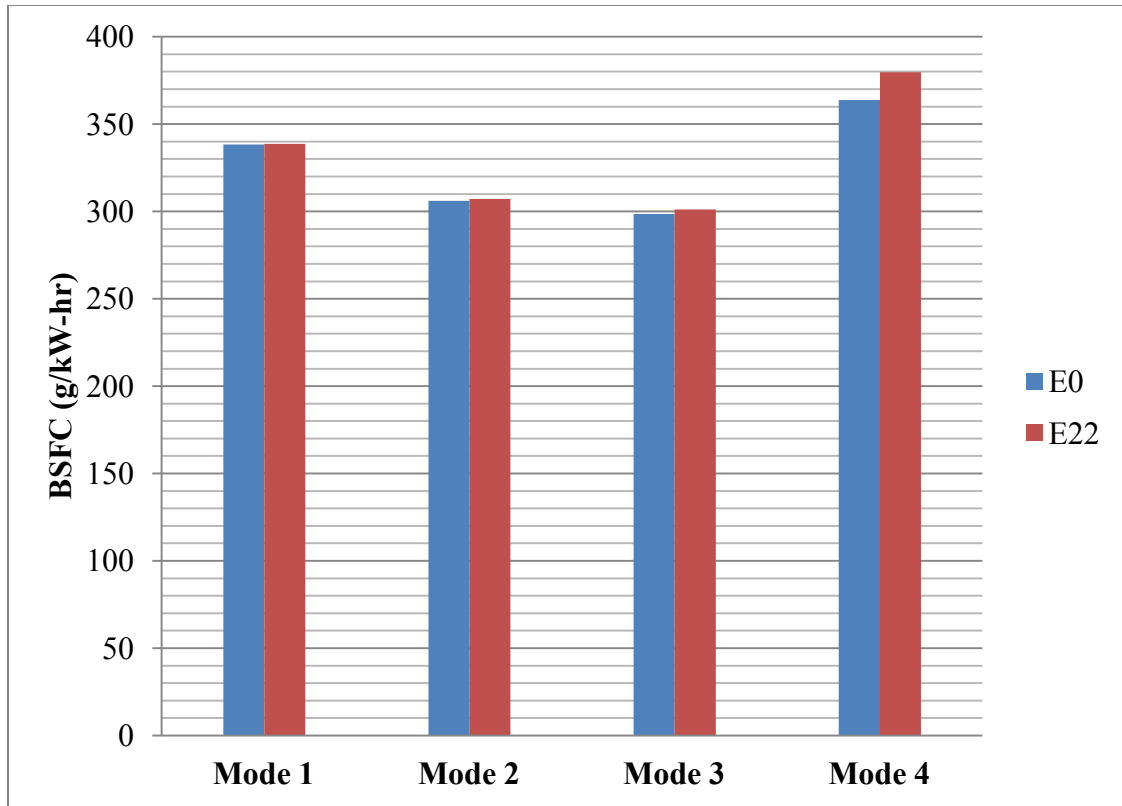
Figure 4.16: Comparison of Arctic Cat brake specific emissions.

Table 4.19

Comparison of Arctic Cat power, fuel flow and BSFC differences from E0 to E22.

Mode	Power Difference (%)	Fuel Flow Difference (%)	BSFC Difference (%)
1	2.0	2.5	0.1
2	0.5	1.3	0.4
3	3.1	4.5	0.8
4	-1.9	3.1	4.4

Figure 4.14 shows the average λ for E0 and E22 for each mode of the Arctic Cat. An average increase of λ of 2.4 % was observed. Modes three and four decreased by 1.2 % and 0.6 % respectively. The largest increase was observed at mode five with a 9.11 % increase. Small changes in λ were observed due to the Arctic Cat's closed-loop fuel

injection system as well as the fuel management system's ability to learn the fuel when operating in mode three.
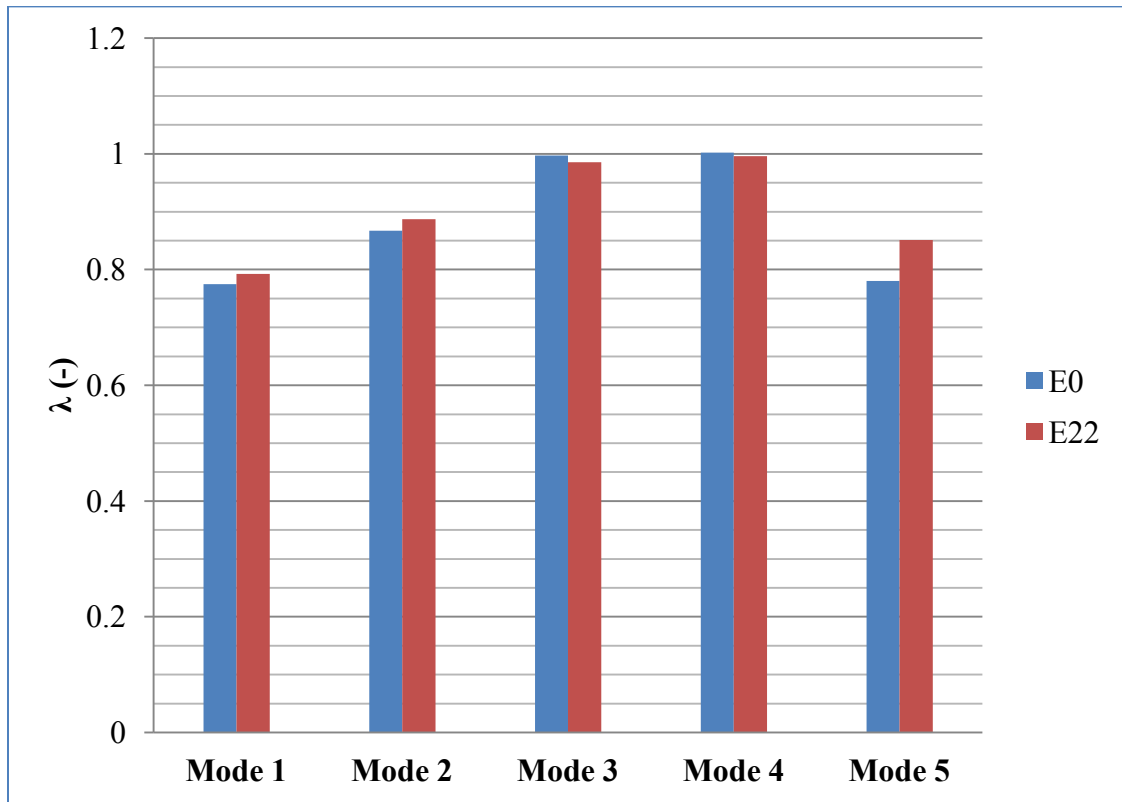

Figure 4.17: Comparison of Arctic Cat relative air/fuel ratio.

4.8.2 Yamaha Apex

Figure 4.15 shows the power of each mode for the Yamaha on each fuel. Again, mode one power was allowed to vary while the other modes were held at a constant torque and engine speed for both fuels.
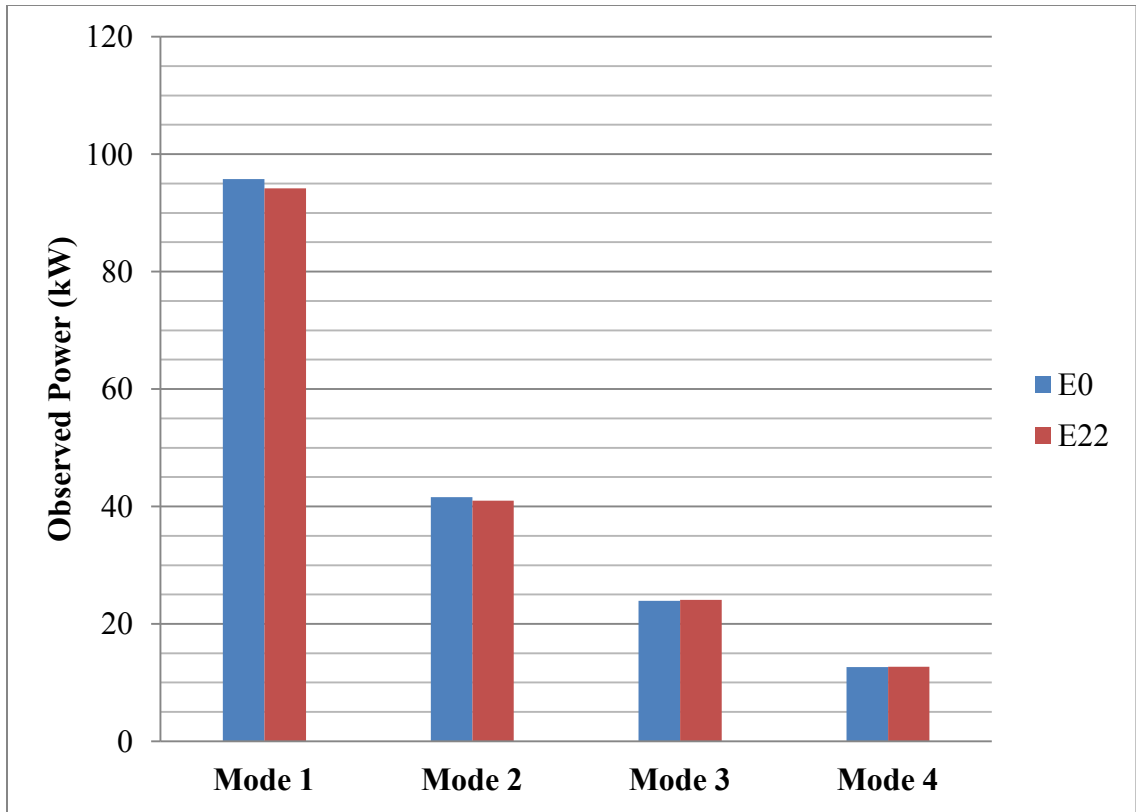
Figure 4.18: Comparison of power at each mode for the Yamaha. Power at each mode should be identical for E0 and E22 for modes two through four.

With the exception of mode two, all of the exhaust gas temperatures increased for E22 (Figure 4.16). Exhaust gas temperatures increased on average by 18° C. This is due to the fuel injection system's inability to adapt to the ethanol concentration which leans out the combustion and moves the AFR closer to the stoichiometric ratio. The leaner combustion overcomes the increased latent heat of vaporization of the ethanol and the exhaust gas temperature increases.
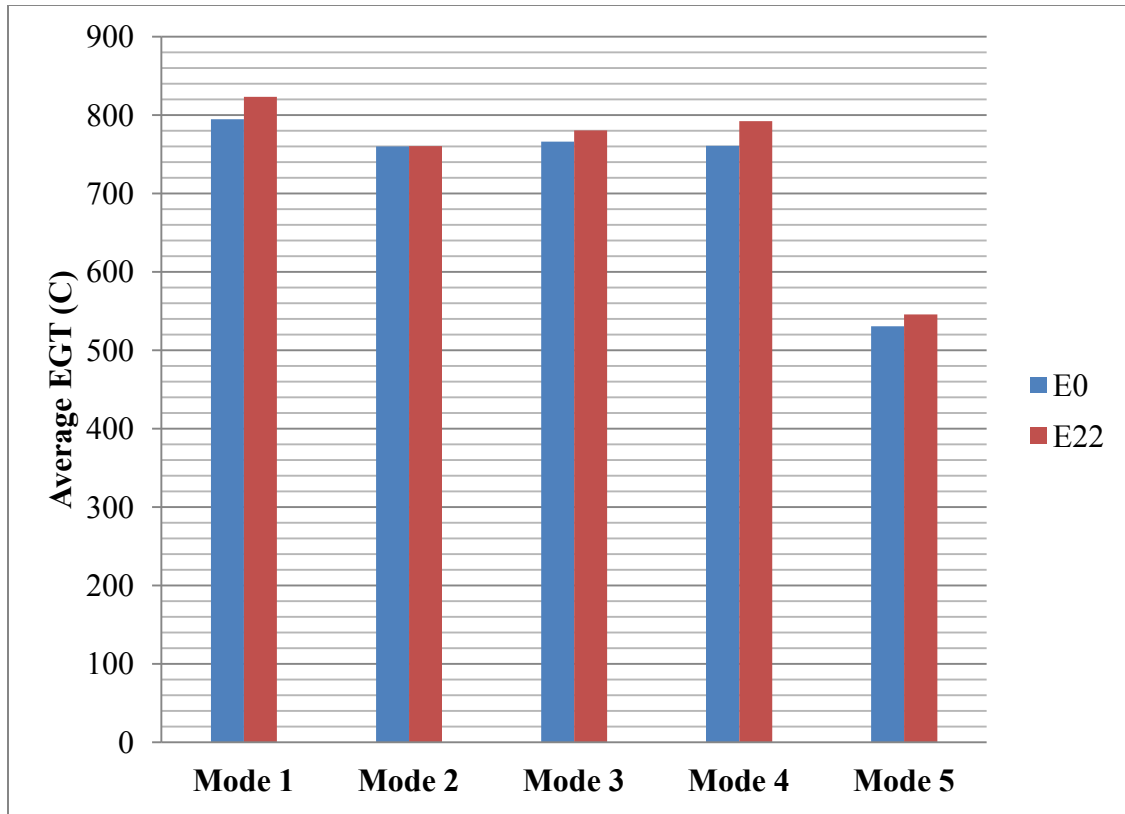
Figure 4.19: Comparison of Yamaha exhaust gas temperature.

A decrease in fuel flow with E22 for mode one was observed (Figure 4.17). This is most likely due to colder ambient temperatures during E0 testing. The ambient temperature during E0 testing was 15.1° C and 28.1° C during E22 testing. Colder ambient temperatures increase the air density which increases fuel delivery. Mode one is affected the greatest as mode one is at wide open throttle. The other modes are less affected as the throttle is merely increased until the same torque is observed. Mode two fuel flow also decreased slightly. This decrease is due to a lower average torque setting for E22. This is confirmed by an increase in BSFC shown in Figure 4.18. Fuel flow for modes three and four increased as expected.
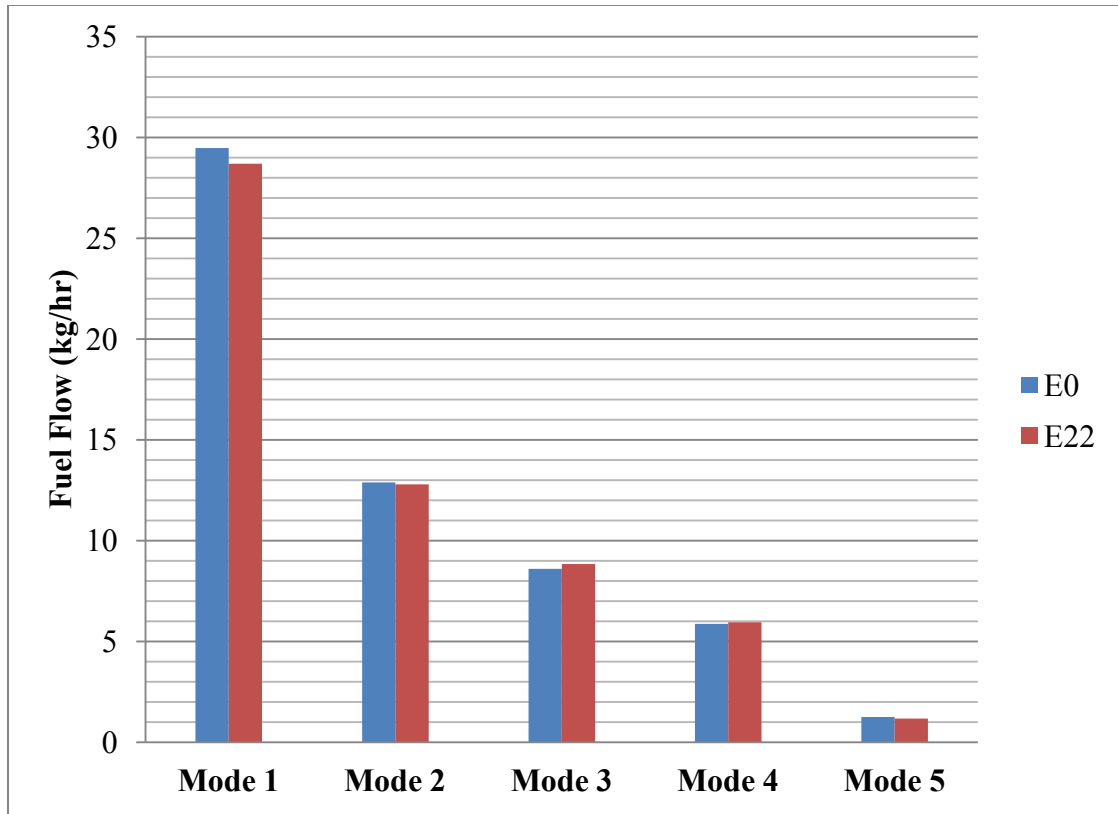
Figure 4.20: Comparison of Yamaha fuel flow.

An increase in BSFC was observed for modes two, three and four (Figure 4.18). Mode one BSFC decreased similarly to the Arctic Cat. In the case of mode one, power and fuel flow decreased by 1.8 % and 2.6 % respectively (Table 4.20). Due to the fact that fuel flow decreased more than power, BSFC decreased. Modes three and four had small increases in power (0.3 % and 0.4 % respectively) with larger increases in fuel flow (2.7 % and 1.3 % respectively) and therefore an increase in BSFC was observed for both modes.
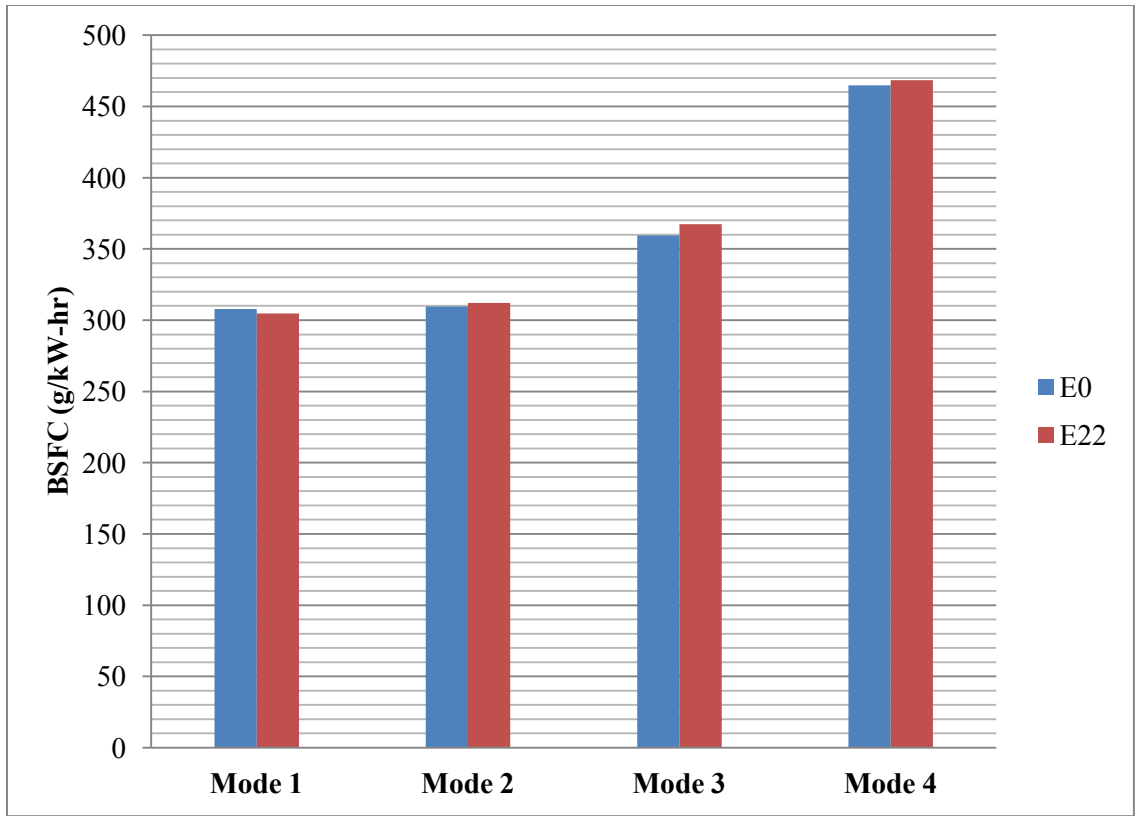
Figure 4.21: Comparison of Yamaha brake specific fuel consumption.

Table 4.20

Comparison of Yamaha power, fuel flow and BSFC differences from E0 to E22.

Mode	Power Difference (%)	Fuel Flow Difference (%)	BSFC Difference (%)
1	-1.8	-2.6	-1.0
2	-1.7	-0.7	0.8
3	0.3	2.7	2.2
4	0.2	1.3	0.8

Figure 4.19 shows the comparison of λ for E0 and E22 for the Yamaha Apex. Relative air/fuel ratio increased for all five modes by an average of 11.8 %. Modes two, three and four went lean of stoichiometric. The leaner combustion was expected due to the increased oxygen content of ethanol.
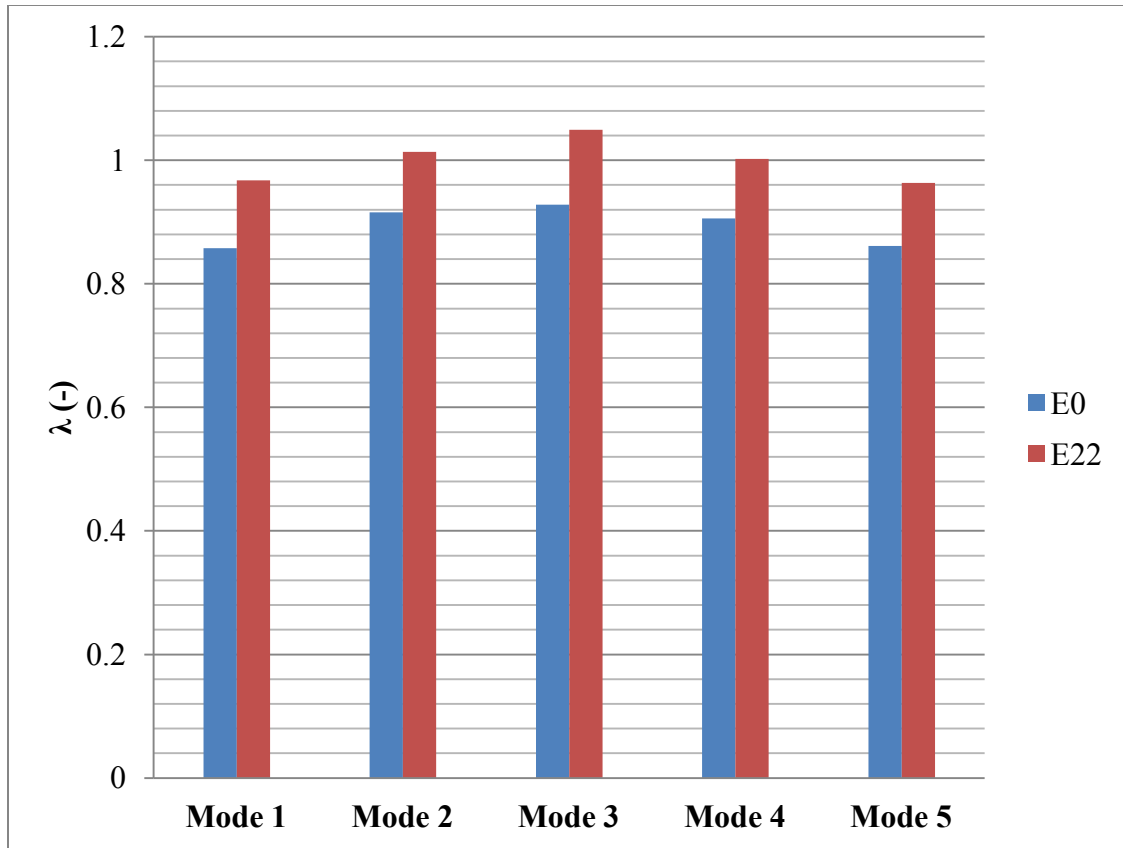
Figure 4.22: Comparison of Yamaha relative air/fuel ratio.

4.8.3 Polaris Rush

Figure 4.20 shows the power at each mode for the Polaris running on both fuels. Mode one (peak power) increased. Modes two through four were held at a constant torque and engine speed for both fuels. Slight differences were observed for modes two through four due to the limits of repeatability of the manually throttle and engine speed control.
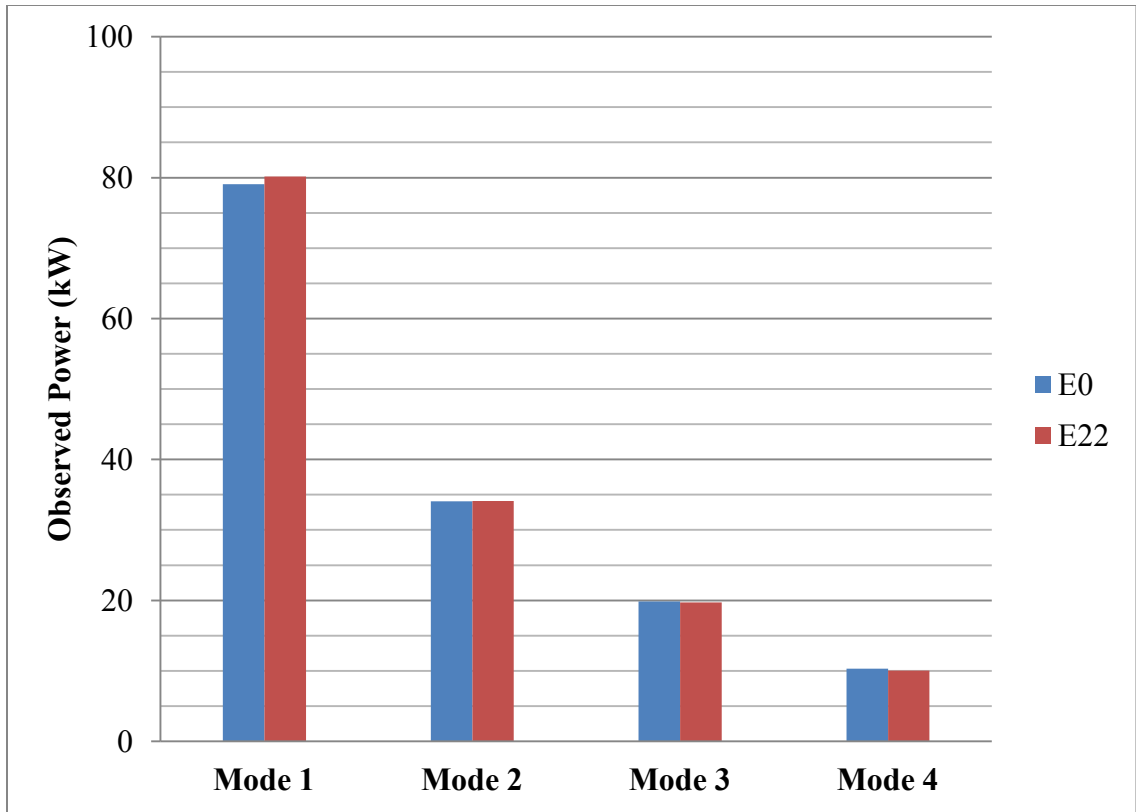
Figure 4.23: Comparison of power at each mode for the Polaris. Power at each mode should be identical for E0 and E22 for modes two through four.

The average exhaust gas temperature increased for all five modes, as shown in Figure 4.21. Exhaust gas temperatures increased on average by 21.2° C. Even though the Polaris had a limited ability to accommodate for ethanol blends (resistor change from E0 to E10), the air/fuel ratio is leaner than calibrated due to the E22 fuel.
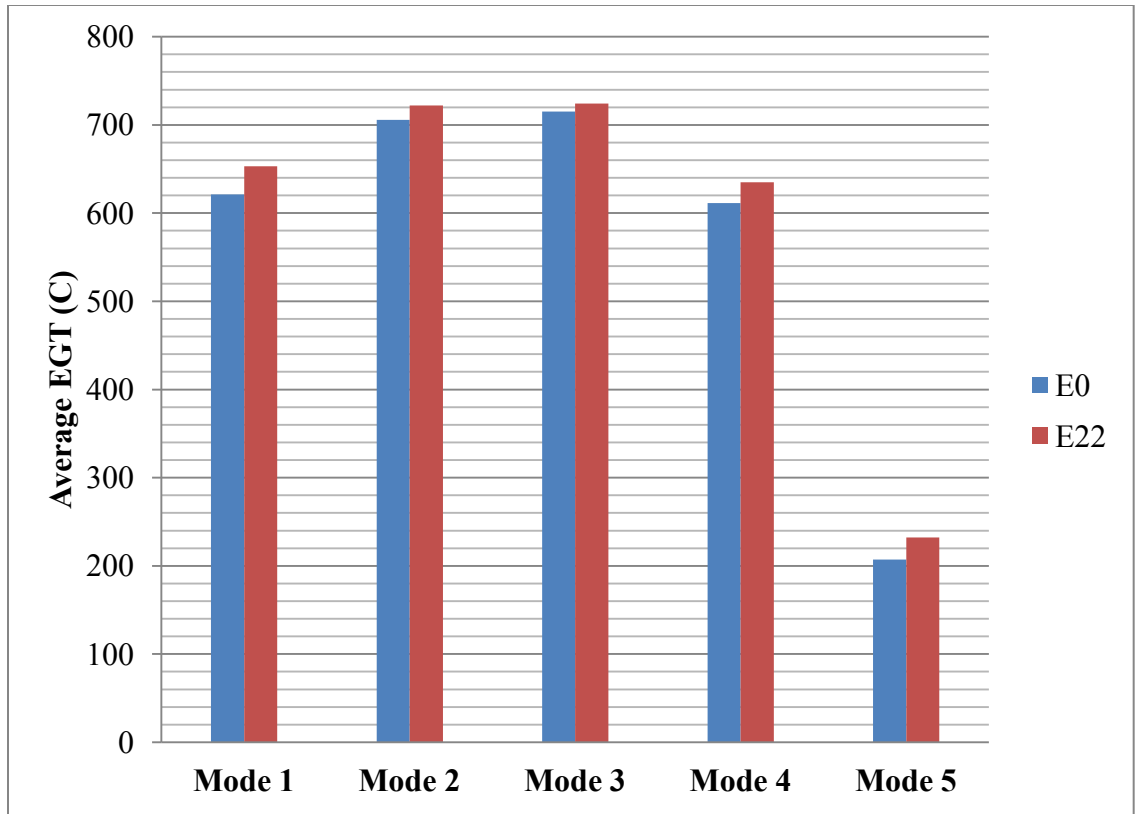
Figure 4.24: Comparison of Polaris exhaust gas temperature.

Figure 4.22 shows an increase in fuel flow for modes one and two as expected. Due to the resistor for E10, fuel flow for mode one should increase by the same percentage of the decrease in energy of E10. There is a 4 % decrease in energy when comparing E10 to E0. Mode one fuel flow increased by 4.6 %. Modes three and five saw a 0.9 % and 1.1 % decrease respectively. A 10.3 % decrease was observed for mode four. This is most likely due to a 3.7 % decrease in torque. This means that the torque was, on average, held low for E22 mode four. The increase in fuel flow at modes one and two is due to the E10 resistor. Fuel delivery is adjusted for E10 at modes one and two to prevent power loss and reduce in-cylinder temperatures. Modes three, four and five are not affected by the resistor change as a decrease in power can be compensated for by increasing the throttle.
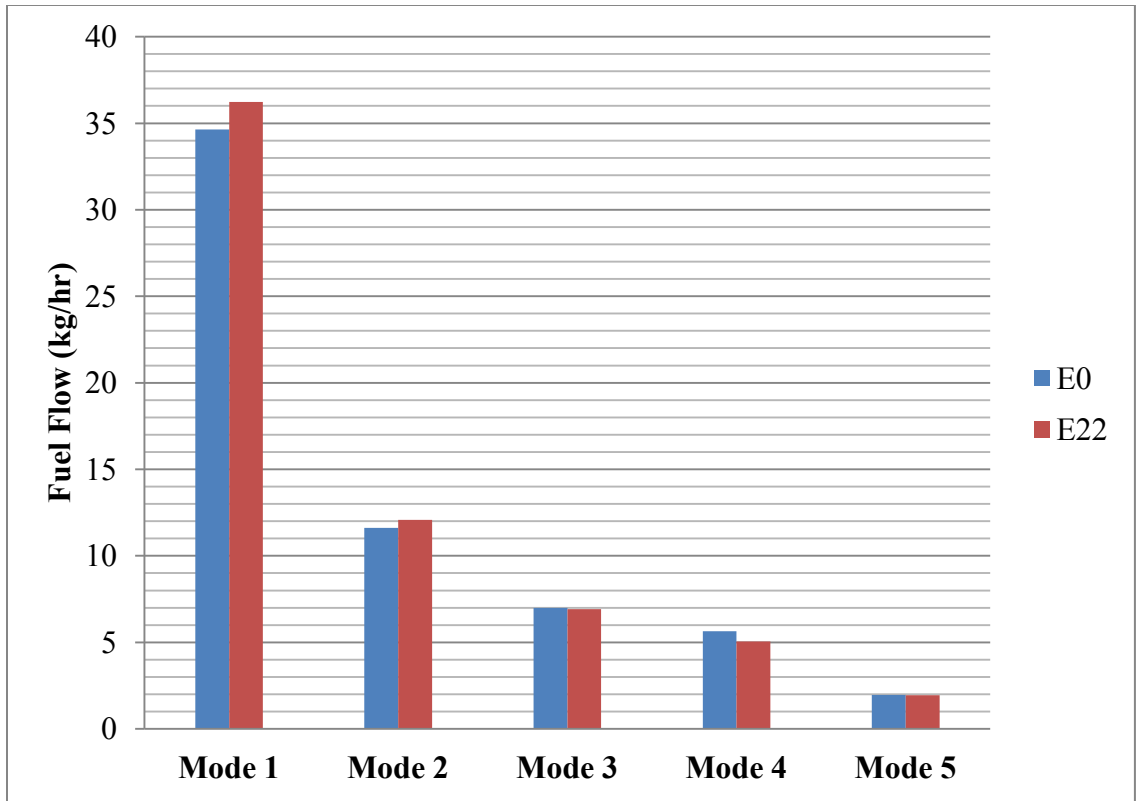
Figure 4.25: Comparison of Polaris fuel flow

Figure 4.23 shows an increase in BSFC for modes one and two, and a decrease for modes three and four. In the case of mode one, the fuel flow increase was larger than the power increase and thus the BSFC increased by 3.2 % (Table 4.21). The same phenomenon occurred for mode two. Modes three and four had a larger decrease of fuel flow (0.9 % and 10.3 % respectively) than that of the power (0.5 % and 2.6 % respectively) and therefore BSFC decreased for both modes (0.3 % and 7.7 % respectively).
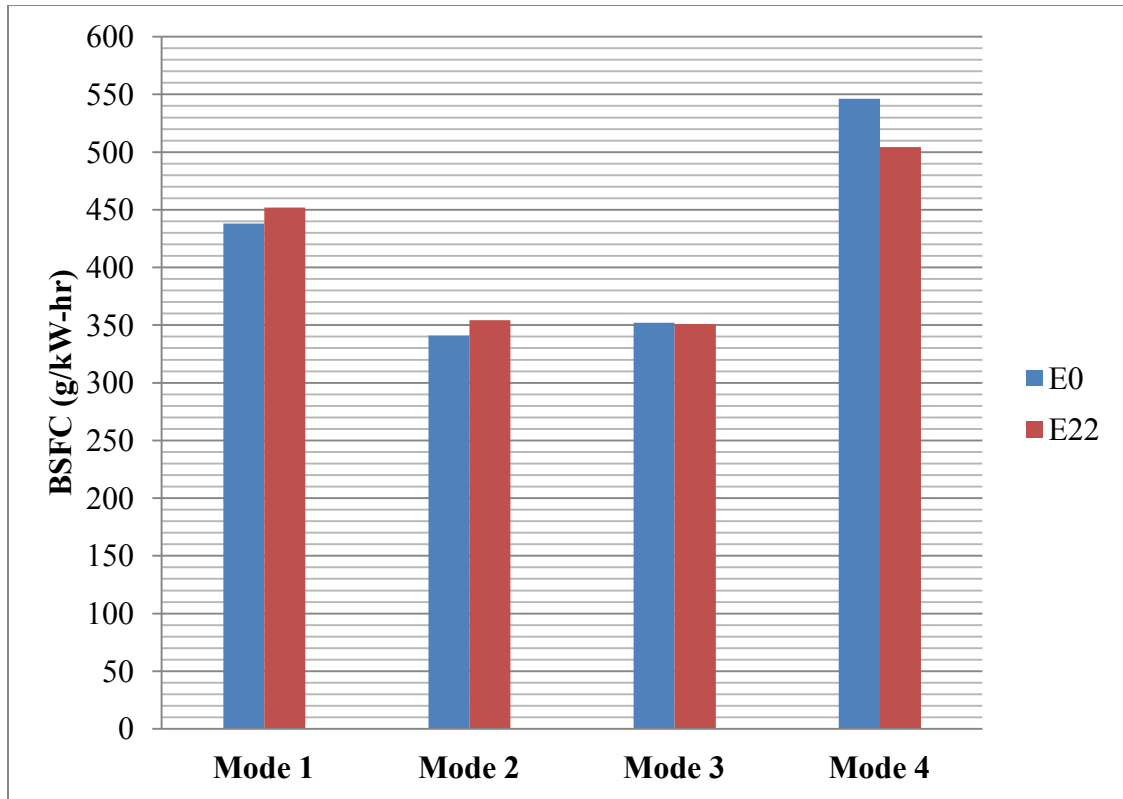
.

Figure 4.26: Comparison of Polaris brake specific fuel consumption.

Table 4.21

Comparison of Polaris power, fuel flow and BSFC differences from E0 to E22.

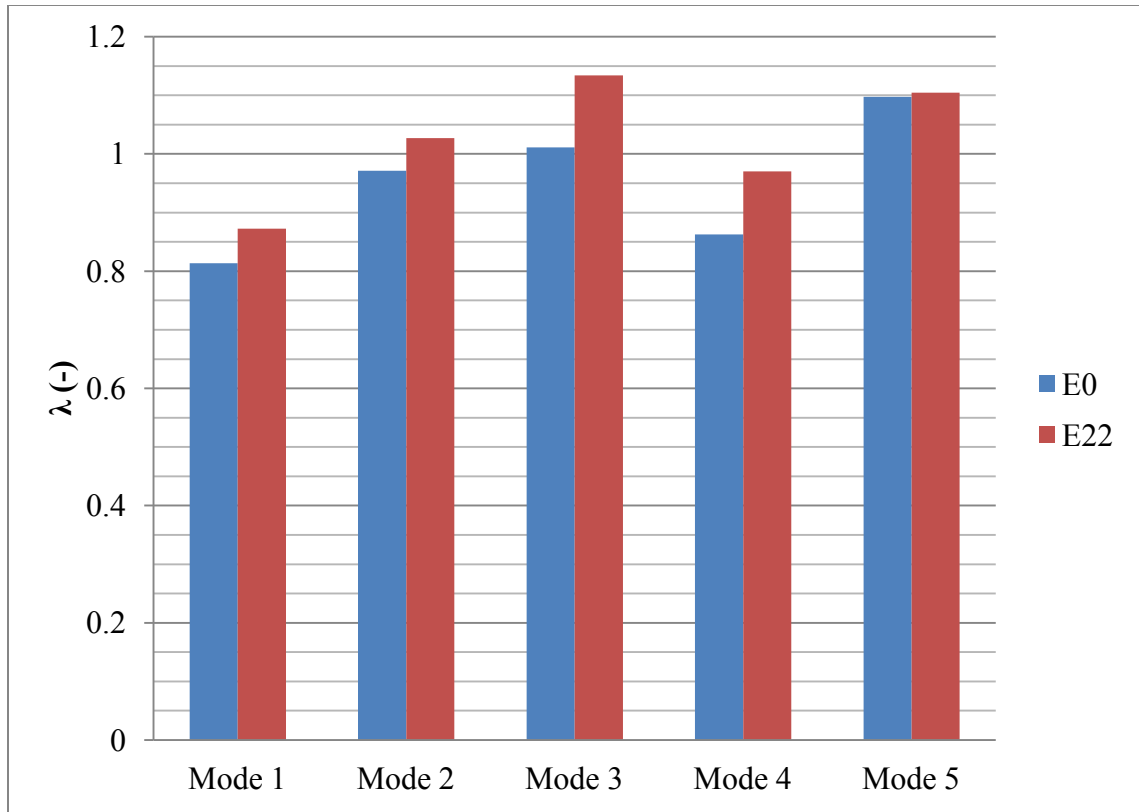| Mode	Power Difference (%)	Fuel Flow Difference (%)	BSFC Difference (%)
1	1.4	4.6	3.2
2	0.2	4.1	4.0
3	-0.5	-0.9	-0.3
4	-2.6	-10.3	-7.7

Figure 4.27: Comparison of Polaris relative air/fuel ratio.

On average, λ increased by 7.6 % for E22 fuel, as shown in Figure 4.24. This is a greater increase than the closed-loop Arctic Cat (2.4 %) and a smaller increase than the open-loop Yamaha (11.8 %). Modes one and two observed a 7.3 % and 5.7 % increase in λ respectively. A larger increase of 12.1 % and 12.5 % occurred at modes three and four respectively. The smaller increase in λ at higher loads is the result of the E10 resistor. The fuel management system compensated for E10 at higher loads to prevent power loss. Due to the fuel having higher ethanol content than 10 % by volume, the AFR was less fuel rich than that of E0.

4.8.4 Engine Performance Comparison Summary

Figure 4.28 shows the average difference of exhaust gas temperature of the E22 fuel compared to E0 fuel. The closed-loop fuel injected Arctic Cat had a 17.6° C average decrease in exhaust gas temperature. This decrease in exhaust gas temperature is due to

the added fuel delivery to maintain a consistent λ. Both open-loop snowmobiles observed an average increase of exhaust gas temperature due enleanment.
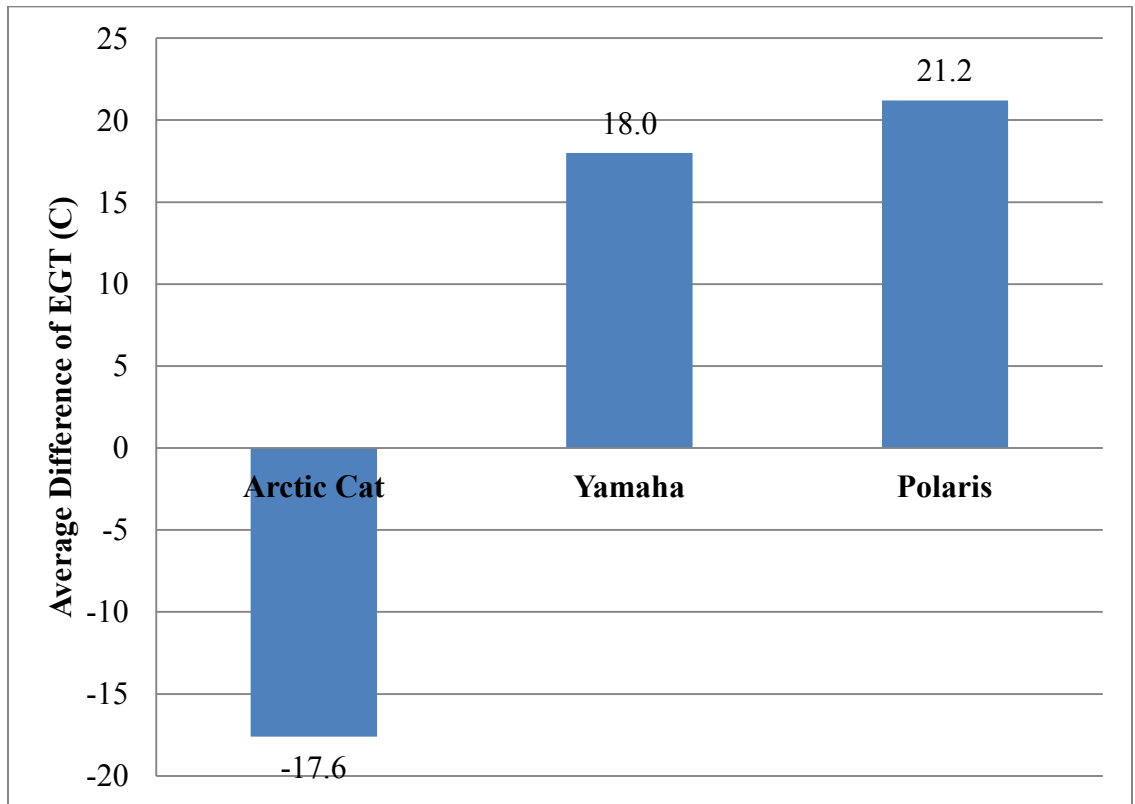

Figure 4.28: Average difference of exhaust gas temperature.

Figure 4.29 shows the average difference of BSFC. An increase of average BSFC was observed for all three snowmobiles. The closed-loop Arctic Cat had the largest increase of average BSFC with a 5.0 g/kW-hr increase. Both the Yamaha and Polaris observed an increase of average BSFC of 2.6 g/kW-hr and 3.8 g/kW-hr respectively.
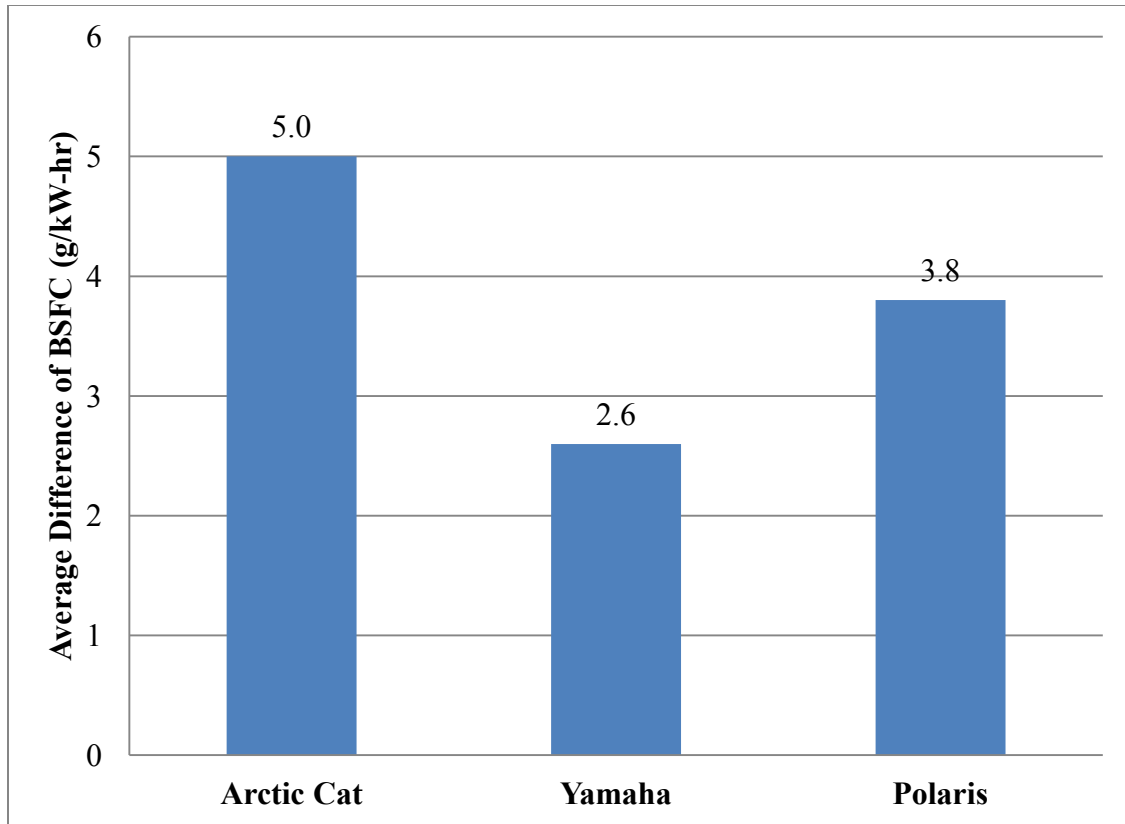
Figure 4.29: Average difference of brake specific fuel consumption.

4.9 Combustion Analysis

Combustion data was only recorded on the Polaris. Figure 4.25 shows the averaged cylinder pressures for all five modes of E0 and E22. The data was then averaged over the two cylinders. Table 4.22 shows the maximum cylinder pressures and the percent change from E0 to E22. Mode one maximum pressure increased by 2.4 %. Mode two peak pressure increased by 1.6 %. Modes three, four and five all saw a decrease in maximum cylinder pressure. The change in resistor for E22 is believed to have caused the increase in peak cylinder pressure. The largest change in the location of the maximum cylinder is a delay of 0.8 CAD at mode four, as shown in Table 4.23.
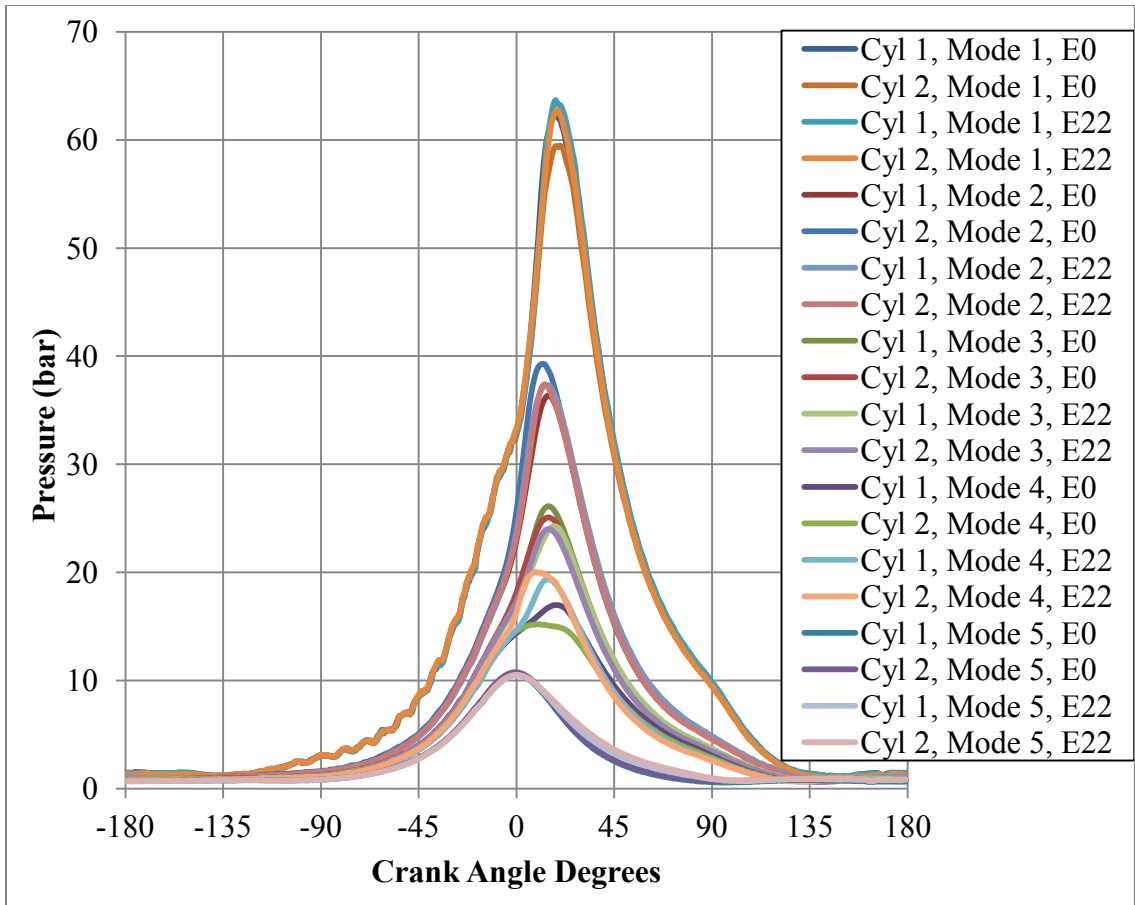
Figure 4.30: Comparison of cylinder pressure traces.

Table 4.22

Comparison of maximum cylinder pressures.

Mode	E0 Pmax (bar)	E22 Pmax (bar)	Difference (%)
1	61.7	63.2	2.4
2	37.3	37.9	1.6
3	25.4	24.4	-3.7
4	15.7	15.3	-2.5
5	11.0	10.7	-2.3

Table 4.23

Comparison of the location of maximum cylinder pressure.

Mode	E0 Angle of Pmax (CAD)	E22 Angle of Pmax (CAD)	Difference (CAD)
1	18.5	18.4	-0.1
2	13.4	13.6	-0.2
3	15.3	16.0	-0.7
4	12.0	11.2	0.8
5	2.3	1.9	0.4

A delay in 50 % MFB was observed for modes three, four and five with E22 fuel (Figure 4.26). 50 % MFB was delayed most significantly for modes three and five by 17.6 % and 152 % respectively. The delay in 50 % MFB is due to an increased combustion duration shown in Figure 4.27.
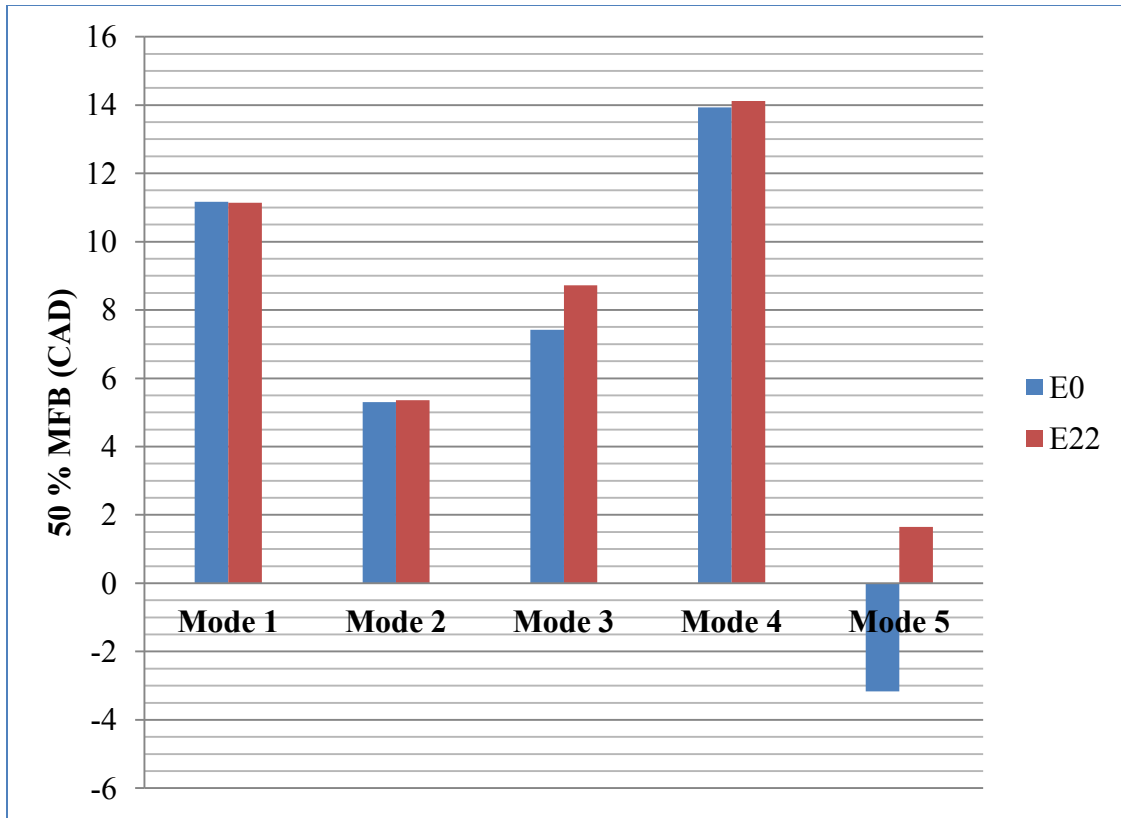
Figure 4.31: Comparison of 50 % mass fraction burn.

Figure 4.27 shows combustion duration from 10 % to 90 % MFB. Combustion duration increased by 7.3 % and 23.7 % for modes three and five, respectively. Modes one, two and four all changed by less than 1 %.
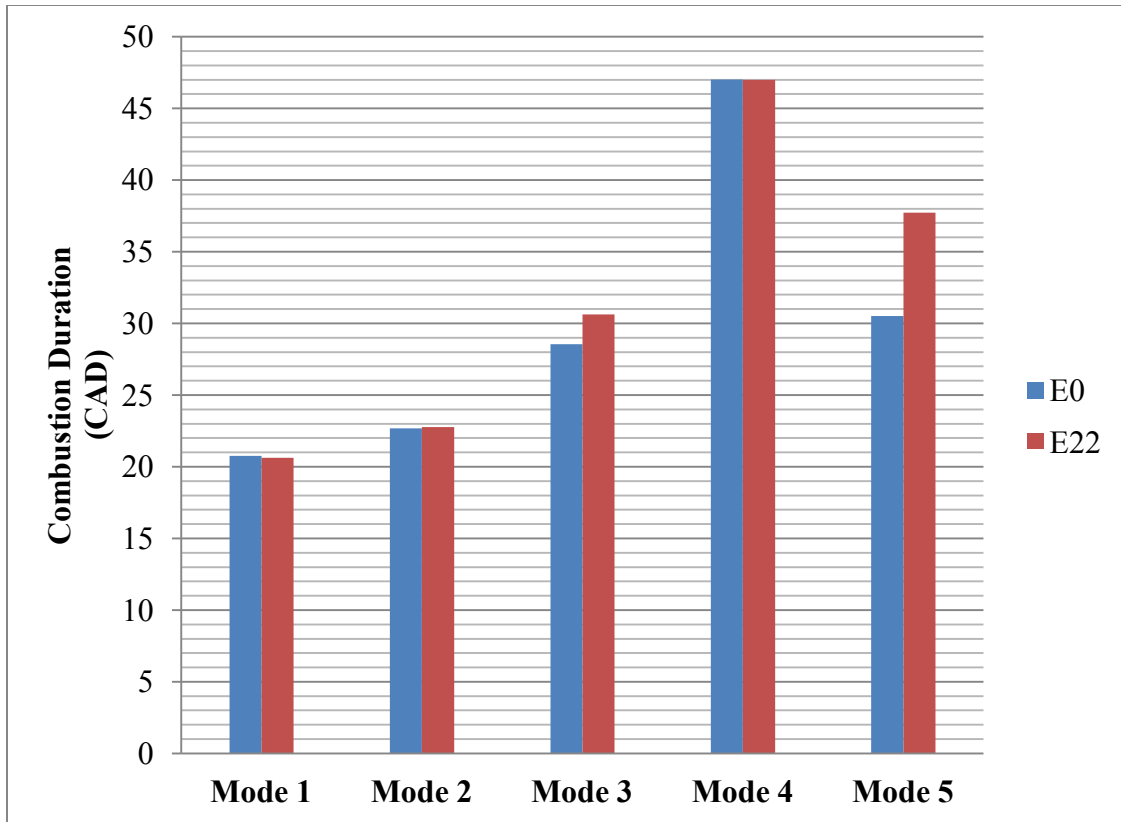
Figure 4.32: Comparison of combustion duration.

IMEP increased for mode one, on average, by 2.4 % (Figure 4.28). A 3.8 % average increase was observed for mode two. IMEP for modes three and four decreased by 1.3 % and 3.7 % respectively. The change in resistor for E22 lead to higher peak cylinder pressures due to additional injection of fuel at modes one and two, as shown in Figure 4.22.
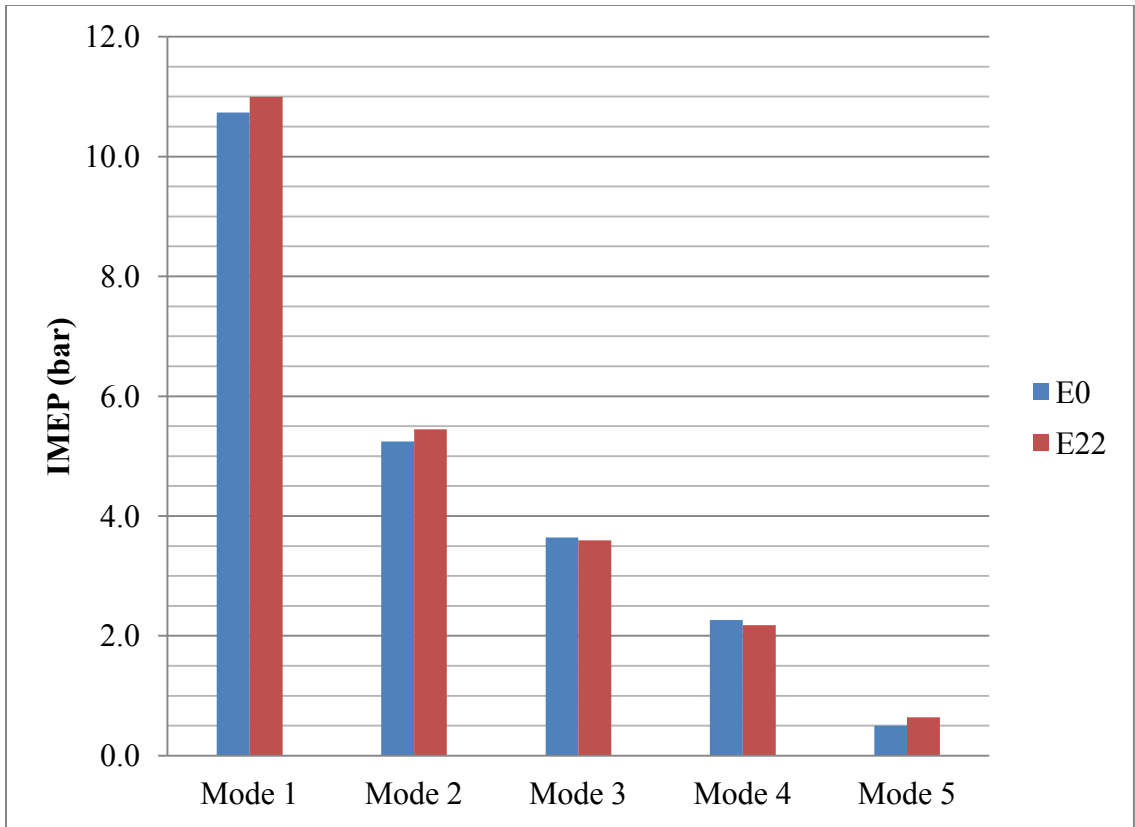
Figure 4.33: Comparison of indicated mean effective pressure.

Chapter 5 Conclusions and Future Work
5.1 Conclusions

Emissions, engine performance and combustion analysis were used to compare the impact of E22 on two-stroke and four-stroke snowmobiles. THC emissions decreased for all three snowmobiles when operating on E22 fuel. CO emissions decreased for all snowmobiles with the exception of the Arctic Cat at mode four which increased by 1.2 %. CO_2 emissions increased for all of the snowmobiles when operating on E22 fuel. The increase in CO_2 and decrease of CO was expected due to the increased oxygen content of the E22 fuel. The oxygenated fuel increases the amount of oxygen available for combustion which promotes more fuel carbon to form CO_2 rather than CO. The closed-loop fuel injection system (Arctic Cat) was able to more accurately maintain the relative air/fuel ratio which reduced cylinder temperatures due to the higher latent heat of vaporization of ethanol.

The closed-loop fuel injection system of the Arctic Cat was able to increase peak brake power by 2.4 %. To obtain the increased power, an increase in fuel flow was observed. The ability of the engine to learn the fuel prevented the AFR from going lean and, as a result, a decrease in exhaust gas temperature was observed. Due to an increase in fuel flow and power, a minimal increase in BSFC was observed for the E22 fuel. The open-loop Polaris engine which was partially able to accommodate the E22 fuel increased peak brake power by 1.4 %. An increase in fuel flow was observed due to the reduced heating value of ethanol. Leaner combustion was also experienced which lead to higher EGTs. A larger increase of fuel flow, compared to the increase in power, occurred at higher loads for the two-stroke Polaris and an increase in BSFC was the result. At lower loads, fuel flow increased less than the power and a decrease in BSFC was observed. The open-loop fuel injection system of the Yamaha was unable to adapt to the ethanol concentration and had a 1.6 % reduction in peak brake power. Leaner combustion resulted in higher EGTs for this snowmobile as well. Warmer ambient temperatures during E22 testing reduced air density and thus decreased fuel flow during mode one. At high loads, fuel flow decreased more than the power for the Yamaha resulting in a

decrease in BSFC for the E22 fuel. At middle to lower loads, fuel flow increased and BSFC increased for the E22 fuel.

Combustion analysis of the Polaris revealed an increase in peak cylinder pressures during modes one and two. Peak cylinder pressures decreased for modes three, four, and five. A significant delay in 50 % MFB and increased combustion duration were observed for mode three. IMEP increased during mode one due to an increase in fuel flow.

5.2 Future Work

A major concern manufacturers and consumers have when operating on higher ethanol content is engine durability. It is suggested that tests be performed to compare both the total life of the engine, as well as, how engine performance and emissions degrade over the life of the engine. Outside of engine performance, maintenance is another concern. The results of this study do not address the effect of ethanol on the durability of other parts necessary for the engine to run, such as the fuel pump, fuel lines and injectors over the life of the engine.

It would also be advised that combustion analysis be conducted on the Arctic Cat and Yamaha. This would be advised, particularly, to compare the effect of the closed and open-loop fuel injection systems, in addition to four-stroke and two-stroke deifferences.

The results of this thesis only covered unaltered production vehicles. It is advised to perform a similar study, but with the engines and fuel management systems optimized for the particular ethanol concentration in the fuel. This includes advancing ignition timing and increasing the compression ratio to capitalize on the anti-knock qualities of ethanol. Direct injection could also potentially benefit from the higher latent heat of vaporization of ethanol. This study could be expanded to include the effects of higher ethanol concentrations and even to determine an optimum concentration for performance and emissions.

Bibliography

1. United States Environmental Protection Agency [Internet]. Renewable Fuel Standard; 2012 [updated 2012 Mar 26, cited 2012 April 13]. Available from: http://www.epa.gov/otaq/fuels/renewablefuels/index.htm

2. International Snowmobile Manufacturers Association (ISMA) [Internet]. Haslett (MI): International Snowmobile Manufacturers Association. Snowmobiling Fact Book [cited 2012 April 13]. Available from: http://www.snowmobile.org/snowmobilefacts.asp

3. Ning L, Manqun L, Bin J, Yongguang Z, Yabing J, Yaqin S, Xicheng Y. 2005. Applicability Investigation of Ethanol Gasoline for Motorcycles. SAE Paper 205-32-0053

4. Knoll K, West B, Huff S, Thomas J, Orban J, Cooper C. 2009. Effects of Mid-Level Ethanol Blends on Conventional Emissions. SAE Paper 2009-01-2723

5. California Environmental Protection Agency, Air Resources Board, "Driving Patterns and Emissions: A New Testing Cycle," Research Notes No. 96-11, (1996).

6. Nakata K, Utsumi S, Ota A, Kawatake K, Kawai T, Tsunooka T. 2006. SAE Paper 2006-01-3380

7. Czerwinski J, Comte P, Makkee M, Reutimann F. 2010. SAE Paper 2010-01-0794

8. Arctic Cat [Internet]. Thief River Falls (MN): Arctic Cat. Arctic Cat TZ1 Turbo Touring LXR; 2012 [cited 2012 April 16]. Available from: http://www.arcticcat.com/snow/sleds/pastModels/2009/TZ1TURBOTOURINGLXR

9. Yamaha Media Website [Internet]. Yamaha; 2012 [cited 2012 April 19]. Available from: http://www.yamaha-motor-media.com/hires.aspx?l=4&m=356&mid=2551&id=9743

10. WASF^{TM} wearesuperfamous [Internet]. We Are Super Famous. Polaris Rush 600 Liberty Engine; 2009 [cited 2012 April 16]. Available from: http://www.wearesuperfamous.com/2009/11/polaris-rush-600-liberty-engine/

11. Pegasus Auto Racing Supplies - Home Page [Internet]. Pegasus Auto Racing Supplies Inc. Big Picture: Optional Clamp Mount for Oxygen Sensor; [cited 2012 April 18]. Available from: https://www.pegasusautoracing.com/bigpicture.asp?RecID=4638

Appendix A

A.1 Additional Plots For Reference

A.1.1 Yamaha E0 CO Repeatability Plots
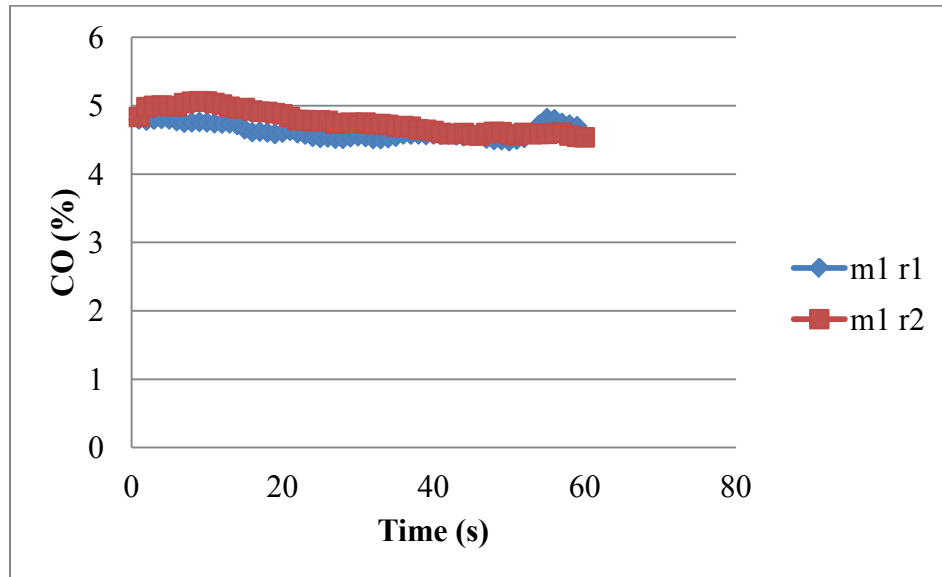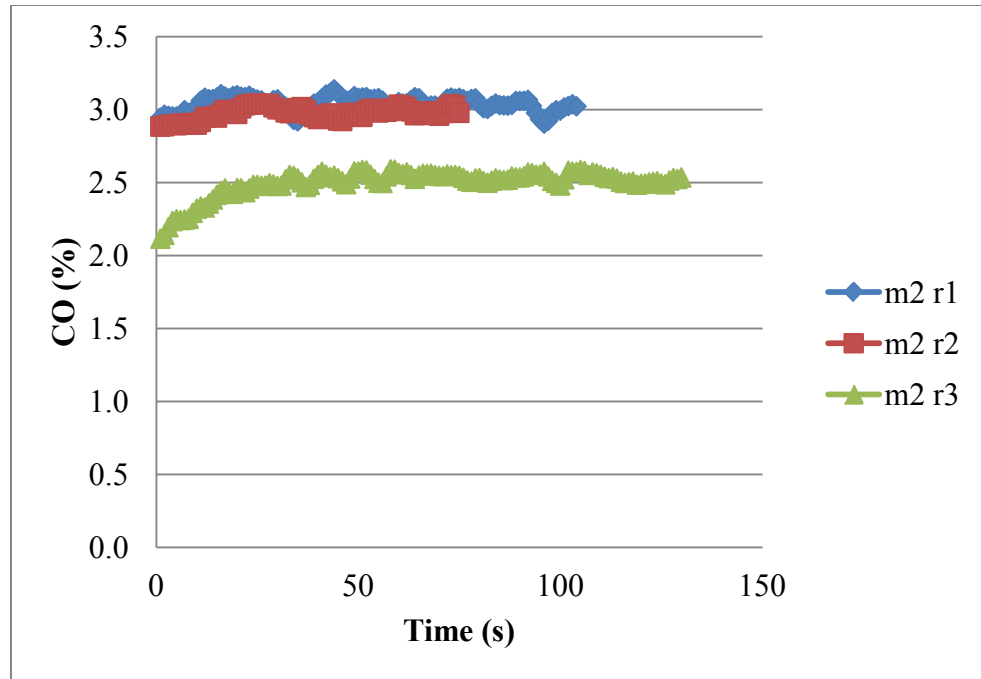
Figure A. 1

Figure A. 2
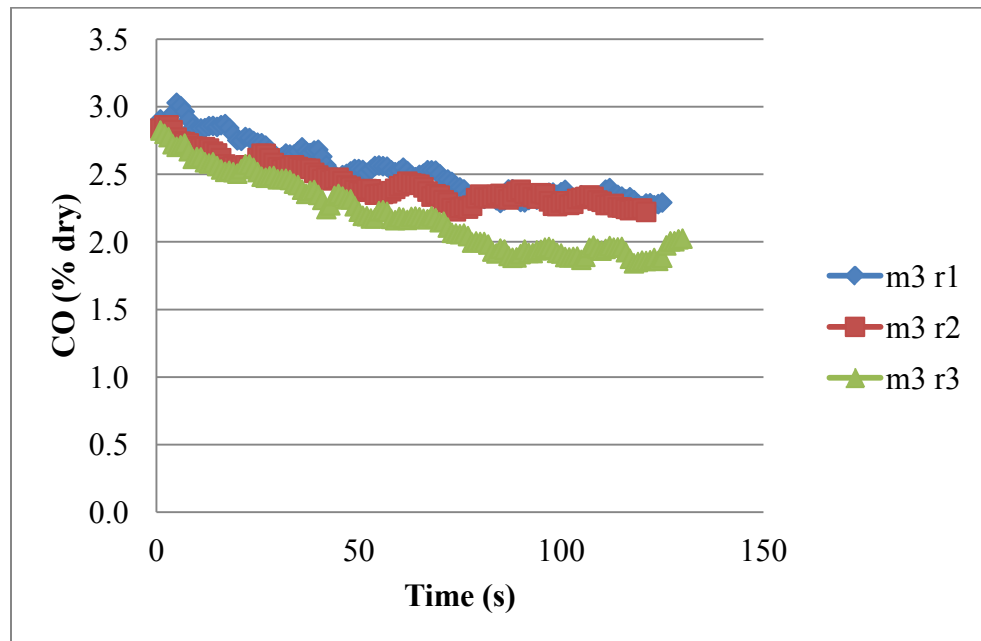
Figure A. 3

Figure A. 4

Figure A. 5

Figure A. 6

Figure A. 7
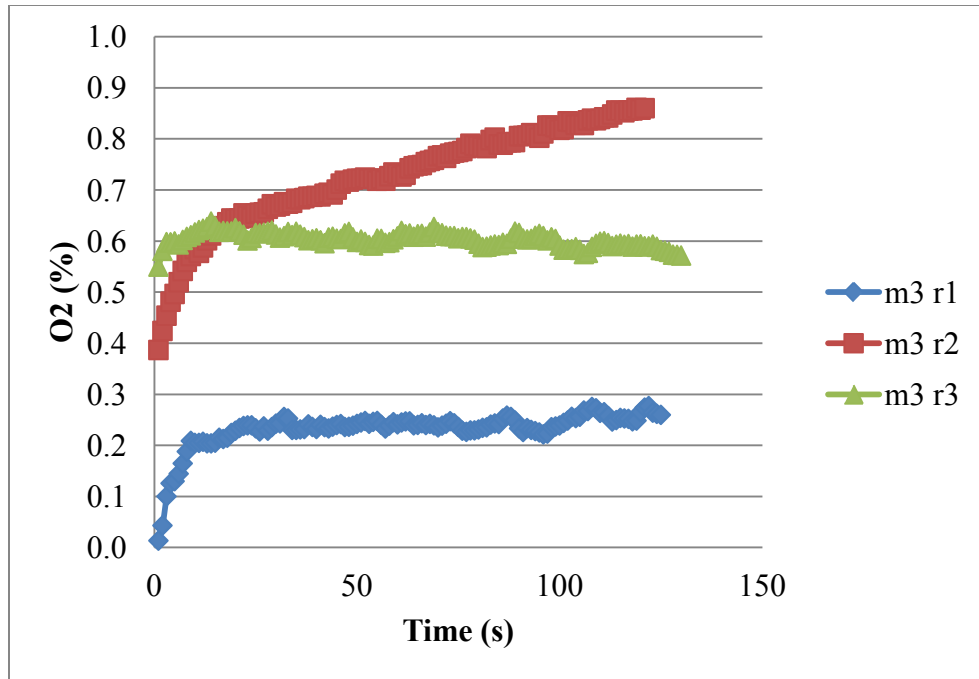
Figure A. 8
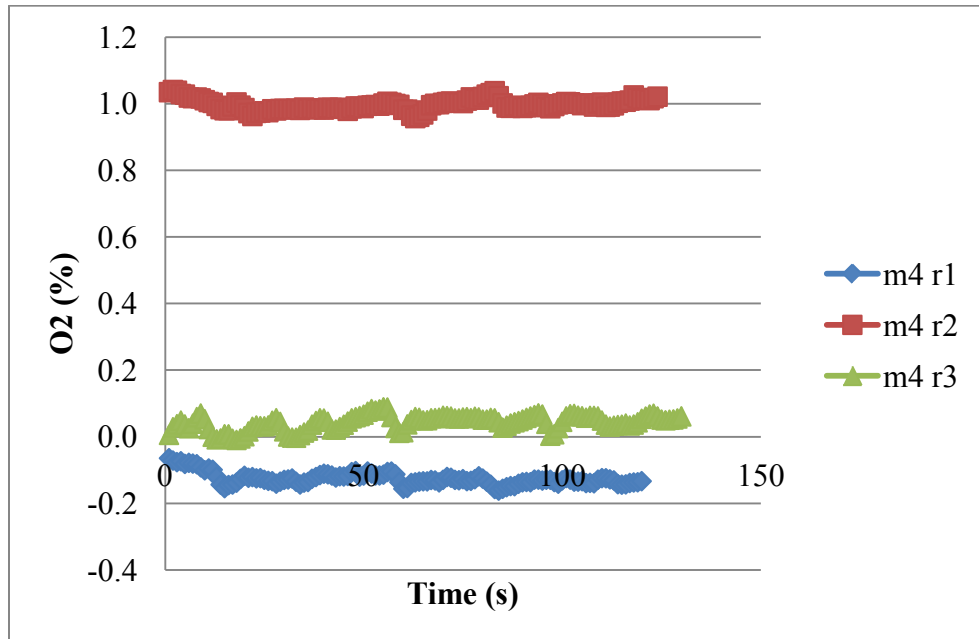
Figure A. 9
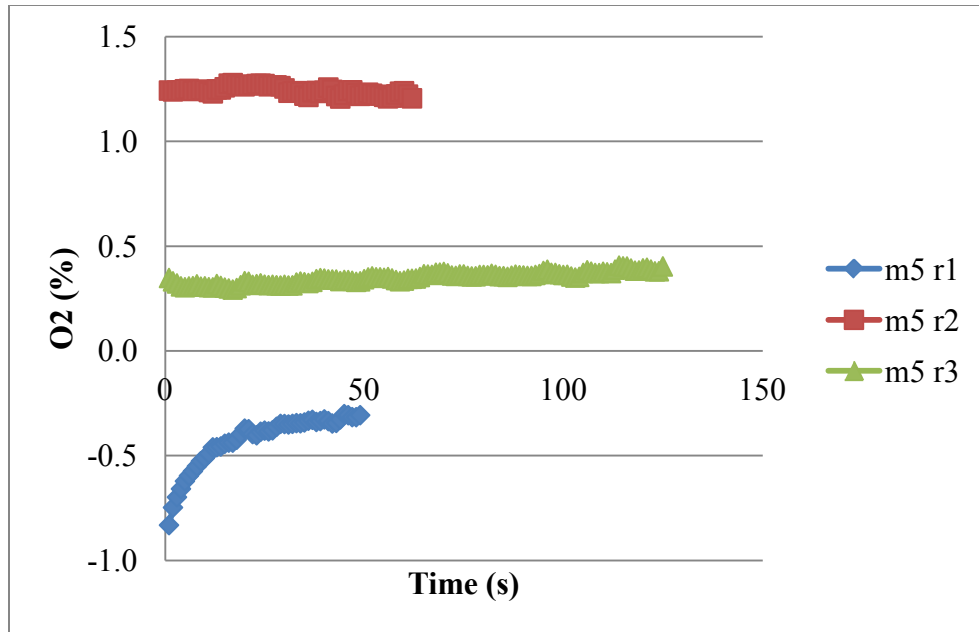
Figure A. 10

A.1.3 Yamaha E0 O_2 Repeatability Plots
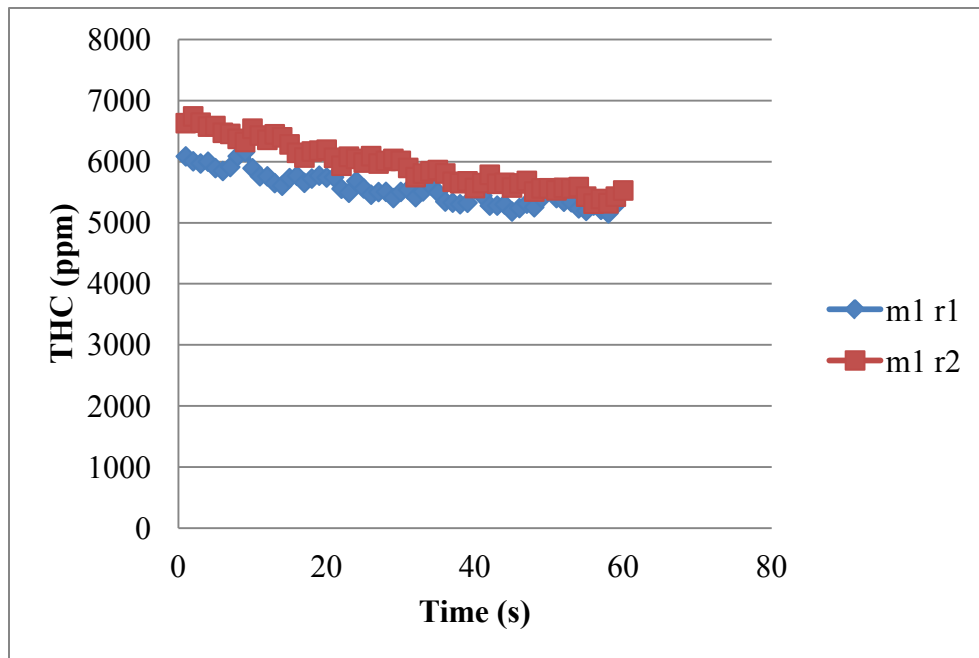
Figure A. 11
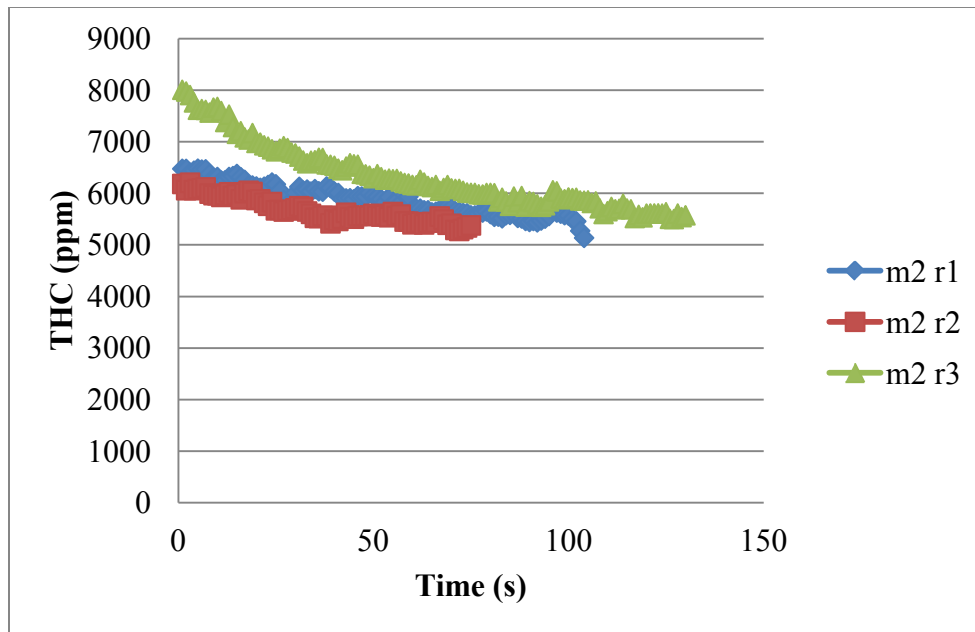
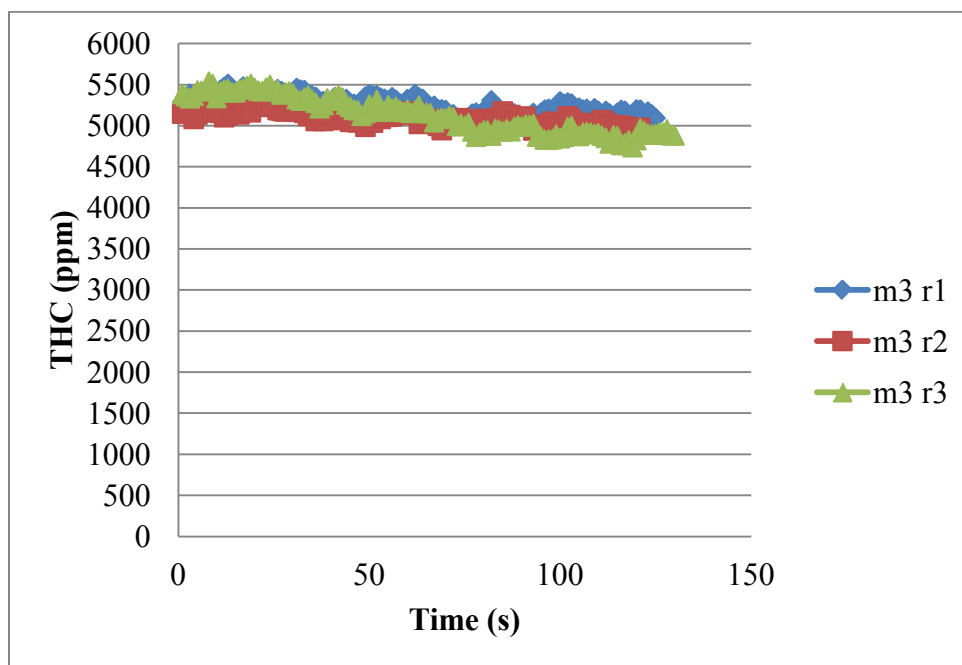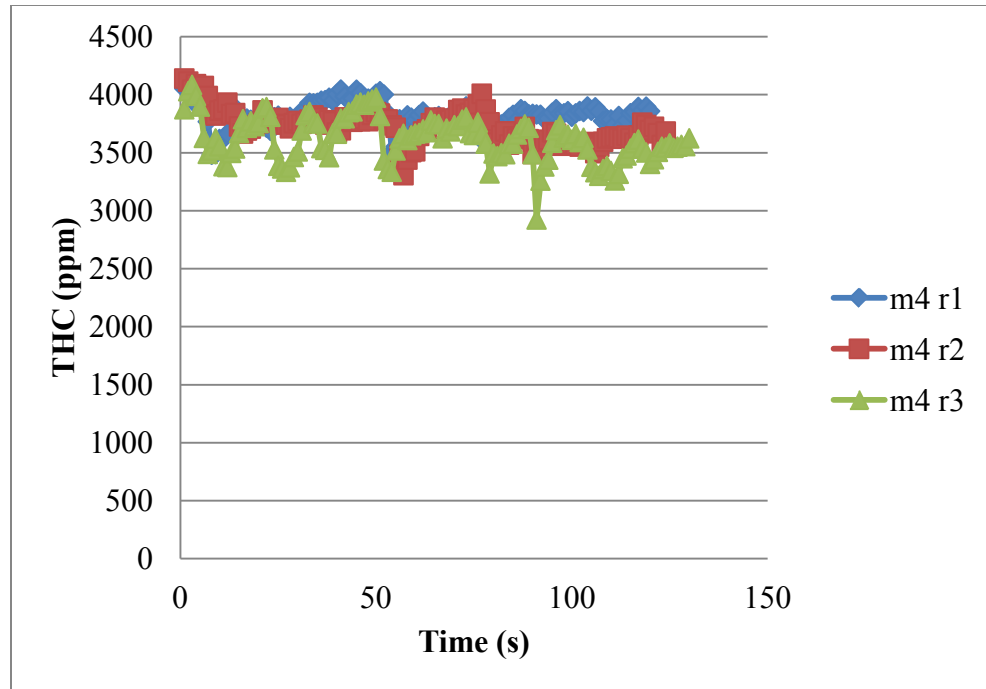**Figure A. 12**

Figure A. 13

Figure A. 14
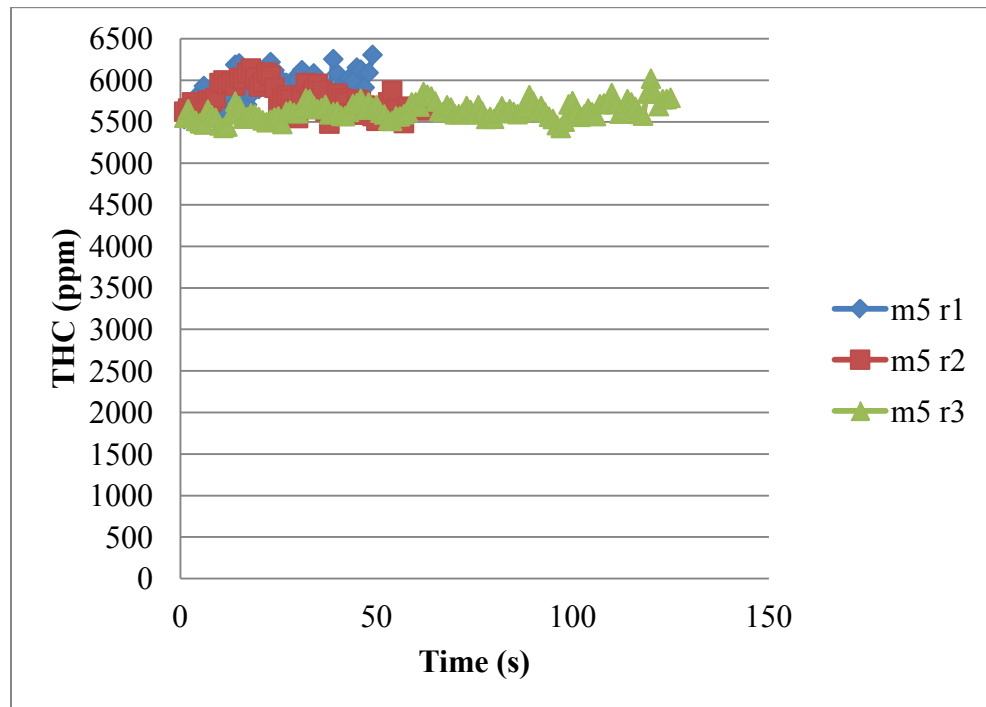
Figure A. 15

A.2   Permissions

A.2.1 Arctic Cat

Hi James,

You have permission to use the Arctic Cat photo providing it does not

provide a negative impression on Arctic Cat products.

Thank you,

Kathy Johnson

Arctic Cat Sales Inc.

218-681-9799 ext. 5504

A.2.2 Pegasus Auto Racing Supplies Inc.

Hi James,

Yes, you have our permission to use that photo for the purpose described below.

Good of luck with your Master's thesis.

Best regards,

Chris Heitman, Co-owner

Pegasus Auto Racing Supplies, Inc.

1-800-688-6946 x1203

Direct: 262-317-1203

Fax: 262-317-1201

Website: www.PegasusAutoRacing.com

----- Original Message -----

From: James Weber

Subject: Permission to reprint picture from website

My name is James Weber and I am writing my thesis for a Master's degree in mechanical engineering at Michigan Technological University. For my research I used the tailpipe clamp mount for oxygen sensor and would like to use the picture of it from your website found at the following link.

I need written permission in order to do so and was hoping this was possible. The title of my thesis is 'Impact of E22 on Two-Stroke and Four-Stroke Snowmobiles'.

https://www.pegasusautoracing.com/bigpicture.asp?RecID=4638

Please let me know if this is possible.

Thank you for your time,

James Weber

A.2.3 Society of Automotive Engineers

Dear Mr. Weber,

Thank you for your correspondence requesting permission to reprint figure 4 from SAE paper 2005-32-0053, figures 10 & 11 from paper 2009-01-2723, and figures 2, 4 & 8 from paper 2006-01-3380 to include in your master's thesis "Impact of E22 On Two-Stroke and Four-Stroke Snowmobiles" for Michigan Technological University.

SAE does not hold the copyright on paper 2009-01-2723. This paper was presented under a US government contract and is in the public domain. You may reprint

this figure and no copyright notice is required. You should reference the authors and SAE paper number in which the figure appeared.

Permission to reprint the figures from papers 2005-32-0053 and 2006-01-3380 is hereby granted, and subject to the following conditions:

Permission is for this one time use only. New requests are required for further use or distribution of the SAE material.

The following credit statement must appear below the figures: "Reprinted with permission from SAE Paper No. XXXXXX* © 200X* SAE International. Further use or distribution is not permitted without permission from SAE." *please insert the paper number and **year of publication

·   This permission does not cover any third party copyrighted work which may appear in the material requested.

Please feel free to contact me if you need further assistance.

Best regards,

Terri Kelly

Intellectual Property Rights Administrator

SAE International| 400 Commonwealth Drive | Warrendale, PA 15096-0001 | USA

Office: +01 724-772-4095 | Fax: +01 724-776-9765

terri@sae.org |www.sae.org

Dear Mr. Weber,

Thank you for your correspondence requesting permission to reprint figures 5, 6-2, 11, 12, 15, and 16 from SAE paper 2010-01-0794 to include in your master's thesis "Impact of E22 On Two-Stroke and Four-Stroke Snowmobiles" for Michigan Technological University.

Permission is hereby granted, and subject to the following conditions:

Permission is for this one-time single use only. New requests are required for further use or distribution of the SAE material.

The following credit statement must appear below the figures: "Reprinted with permission from SAE Paper No. 2010-01-0794 © 2010 SAE International. Further use or distributionis not permitted without permission from SAE."

· This permission does not cover any third party copyrighted work which may appear in the material requested. If this material originated from another source, you must contact the original copyright holder for this permission.

Again, thank you for contacting SAE for this permission.

Best regards,

Terri Kelly

Intellectual Property Rights Administrator

SAE International| 400 Commonwealth Drive | Warrendale, PA 15096-0001 | USA

Office: +01 724-772-4095 | Fax: +01 724-776-9765

terri@sae.org |www.sae.org